Deliverable D2.3

Report on electrochemical testing of new, spent and recycled cells

Funded by the European Union

Views and opinions expressed are those of the author(s) only and do not necessarily reflect those of the European Union or CINEA. Neither the European Union nor the granting authority can be held responsible for them. This project has received funding from Horizon Europe research and innovation programme under Grant Agreement No.1069890

Feasible Recovery of critical raw materials through a new circular Ecosystem for a Li-Ion Battery cross-value chain in Europe

WP2 - End-of-life LIBs Collection and Characterisation, Digital Tools and Battery Passports deployment

D2.3 - Report on electrochemical testing of new, spent and recycled cells

Due date of deliverable	**Actual submission date:**	Organisation name responsible for this deliverable: NESSTEC
28/02/2025	11/03/2025	

Dissemination Level

SEN	Sensitive	
PU	Public	X

Project Acronym FREE4LIB
Grant Agreement No. 101069890
Project Start Date 01-09-2022
Project End Date 31-08-2026
Duration 48 months

Funded by the European Union

Views and opinions expressed are those of the author(s) only and do not necessarily reflect those of the European Union or CINEA. Neither the European Union nor the granting authority can be held responsible for them. This project has received funding from Horizon Europe research and innovation programme under Grant Agreement No.1069890

Disclaimer

Free4lib is an EU-funded project that has received funding from the European Union's Horizon Europe research and innovation programme under grant agreement no. 101069890. The sole responsibility for the content of this report lies with the authors. It does not necessarily reflect the opinion of the European Union. The European Commission is not responsible for any use that may be made of the information contained therein.

Versions

DATE	VERSION	AUTHOR	COMMENT
18/02/2025	1	NESSTEC, FBK, SAKARYA, IREC	First draft of the document
05/03/2025	2	Mattia Duranti, Maheandar Manokaran	Second draft of the document
09/03/2025	3	Martin Weinzerl, Danial Karimi, Daniel Horn	Comments from WP2
10/03/2025	4	NESSTEC, FBK, SAKARYA, IREC	Final document

Contents

Funded by the European Union

Views and opinions expressed are those of the author(s) only and do not necessarily reflect those of the European Union or CINEA. Neither the European Union nor the granting authority can be held responsible for them. This project has received funding from Horizon Europe research and innovation programme under Grant Agreement No.1069890

Funded by the European Union

Views and opinions expressed are those of the author(s) only and do not necessarily reflect those of the European Union or CINEA. Neither the European Union nor the granting authority can be held responsible for them. This project has received funding from Horizon Europe research and innovation programme under Grant Agreement No.1069890

List of Abbreviations

ACRONYMS	DESCRIPTION
Ah	Ampere-hour
C-Rate	Charge/Discharge Rate
CV	Cyclic Voltammetry
DEC	Diethyl Carbonate
DMC	Dimethyl Carbonate
EC	Ethylene Carbonate
EOL	End-of-Life
LFP	Lithium Iron Phosphate
LIB	Lithium-Ion Battery
$LiPF_6$	Lithium Hexafluorophosphate
LMNO	Lithium Manganese Nickel Oxide
mAh/g	Milliampere-hour per gram
Ni	Nickel
NMC	Nickel Manganese Cobalt Oxide
OCV	Open Circuit Voltage
PEIS	Potentio Electrochemical Impedance Spectroscopy
PVDF	Poly(vinylidene fluoride)
SEI	Solid Electrolyte Interphase
SOC	State of Charge
SOH	State of Health
Super P	Conductive Carbon Additive
XRD	X-Ray Diffraction

Funded by the European Union

Views and opinions expressed are those of the author(s) only and do not necessarily reflect those of the European Union or CINEA. Neither the European Union nor the granting authority can be held responsible for them. This project has received funding from Horizon Europe research and innovation programme under Grant Agreement No.1069890

1. Executive summary

This deliverable presents the electrochemical characterization of new, spent, and recycled lithium-ion battery (LIB) cells to assess their potential for second-life applications and material recovery. The study evaluates end-of-life (EOL) battery cells sourced from electric vehicles, e-bikes, and e-scooters, analyzing their remaining capacity, internal resistance, and cycling stability. These diagnostic assessments inform decisions regarding their suitability for reuse or direct recycling, contributing to the development of sustainable battery management strategies.

Battery cells that are unsuitable for second-life applications have been subjected to recycling processes, leading to the reassembly of new cells incorporating recycled electrode materials. The physical, structural, and morphological characterizations of these materials were detailed in previous deliverables. This report focuses on the electrochemical performance of newly assembled lithium-ion cells, tested at both the coin and pouch cell levels. Through impedance spectroscopy, cyclic voltammetry, and galvanostatic charge-discharge cycling, these tests provide critical insights into the efficiency of material recovery processes and the feasibility of integrating recycled materials into new battery production.

Furthermore, the scale-up of LIBs to pouch cell configurations was conducted to evaluate the transition from laboratory-scale testing to commercially relevant formats. Optimized pouch cells with dimensions of approximately 12 cm × 7 cm and an average capacity of 7 Ah were assembled using commercial materials as a benchmark. After optimizing the recycled materials, new pouch cells of identical dimensions will be fabricated and tested to assess their practical viability. These efforts support the project's goal of establishing a circular economy for LIBs, minimizing environmental impact, and reducing dependency on critical raw materials.

The findings from this deliverable will contribute to WP4, aiding in the development of large-scale re-manufacturing strategies and battery pack designs. The results obtained serve as a foundation for future advancements in LIB recycling technologies, reinforcing the importance of sustainable practices in the battery industry.

Funded by the European Union

Views and opinions expressed are those of the author(s) only and do not necessarily reflect those of the European Union or CINEA. Neither the European Union nor the granting authority can be held responsible for them. This project has received funding from Horizon Europe research and innovation programme under Grant Agreement No.1069890

2. Introduction

The increasing demand for lithium-ion batteries (LIBs) in electric vehicles (EVs), portable electronics, and renewable energy storage has raised concerns regarding the sustainability of raw material extraction and battery waste management. LIBs contain valuable materials such as lithium, cobalt, nickel, and graphite, which are limited in supply and require energy-intensive extraction processes. End-of-life (EOL) battery management has become a critical challenge, necessitating the development of efficient recycling and reuse strategies to minimize environmental impact and reduce dependency on primary resources.

Recent studies have explored the potential of reusing EOL battery cells for secondary applications, such as energy storage systems for renewable grids and stationary applications. The feasibility of second-life batteries depends on their remaining capacity, degradation mechanisms, and safety performance. Various electrochemical characterization techniques, including capacity fade analysis, impedance spectroscopy, and cycle life testing, have been employed to assess the viability of second-life applications.

In addition to second-life use, the recovery and reuse of electrode materials have gained significant attention. Studies have shown that recycled lithium-iron-phosphate (LFP) and nickel-manganese-cobalt (NMC) cathodes can exhibit comparable electrochemical performance to commercially manufactured materials when properly processed. Key challenges include impurity control, structural integrity retention, and the optimization of electrode manufacturing processes using recovered materials. Advances in material recovery and reassembly methods, particularly in scalable processes, are crucial for the commercial viability of recycled LIBs.

The global LIB recycling market has experienced significant growth, driven by regulatory frameworks, resource scarcity, and increasing EV adoption. Europe has implemented stringent policies, including the EU Battery Regulation, which mandates high recycling efficiency and sustainable material sourcing. Major battery manufacturers and technology companies are investing in recycling facilities to ensure a stable supply of critical materials.

While the demand for LIBs is expected to grow exponentially, concerns regarding raw material shortages and geopolitical dependencies underscore the importance of establishing a robust recycling infrastructure. The economic feasibility of LIB recycling depends on technological advancements, government incentives, and the scale-up of efficient processing methods.

Funded by the European Union

Views and opinions expressed are those of the author(s) only and do not necessarily reflect those of the European Union or CINEA. Neither the European Union nor the granting authority can be held responsible for them. This project has received funding from Horizon Europe research and innovation programme under Grant Agreement No.1069890

The FREE4LiB project plays a crucial role in addressing the challenges associated with LIB end-of-life management by evaluating the electrochemical performance of used battery cells, assessing the feasibility of second-life applications, and validating the use of recycled materials in new battery production. The results obtained will contribute to the optimization of recycling methodologies and the development of high-performance LIBs with sustainable material sourcing.

By demonstrating the viability of reusing spent batteries and incorporating recycled materials into newly assembled cells, this project supports the EU's strategic objectives in promoting circular economy practices and reducing reliance on critical raw materials. The findings will not only facilitate advancements in battery recycling technologies but also provide valuable insights for industry stakeholders involved in battery manufacturing, energy storage solutions, and policy development.

3. Testing of End-Of-Life Cells (FBK)

3.1 Standard Testing Procedure

3.1.1 Development Context

In order to perform characterization within the FREE4LIB project, FBK developed a procedure specifically suited for testing End-of-Life (EoL) cells and cells manufactured from commercial or recycled materials. This procedure was developed considering that the cells under testing might be in very poor performance conditions, therefore it is also suited for characterizing cells out of datasheet specifications, or showing a very low State of Health (SoH).

The procedure was developed in several versions, as a consequence of the different steps of a trial-and-error process. The first and several other versions have been shared for review, therefore comments and suggestions from all the partners of Task 2.2 have been embedded along the process.

The scope of the testing activity for which the procedure has been developed are:

- Identification of the state of the cell with respect to nominal or expected specifications
- Recording of data useful for the identification of parameters to be used in lumped models of LIB cells developed in T2.3
- Recording of data suitable for the validation of lumped models of LIB cells developed in T2.3

Funded by the European Union

Views and opinions expressed are those of the author(s) only and do not necessarily reflect those of the European Union or CINEA. Neither the European Union nor the granting authority can be held responsible for them. This project has received funding from Horizon Europe research and innovation programme under Grant Agreement No.1069890

The procedure has been developed taking for reference the standard IEC 62660-1, but applying important modifications to meet the needs of the FREE4LIB project. In fact, in the project context, the procedure has to be applied to a large amount of cells by different partners, which have different equipment and time constraints. Therefore, the developed procedure has the following features:

- Possibility to test cells with very different nominal specifications
- Possibility to test cells with very different health conditions
- Alternative options for short and extensive testing
- Possibility to test either in thermally controlled environment, or in ambient conditions

3.1.2 Procedure Description

The final version of the procedure is attached to this document as Annex A.

The procedure is structured in 5 sections:

1. **Preconditioning** - Preliminary cycling of the cell (2 cycles) with first measurement of the cell capacity (Q_exp_pre) and definition of the SoC (SoC_pre).
2. **Open Circuit Voltage (optional)** - One cycle al very low C-rate, providing information for the calculation of the OCV vs SoC curve. OCV can be calculated as the average of charging and discharging voltage at the same SoC.
3. **Energy & Capacity** - Cycling at different C-rates, with identification of the discharge capacity and definition of state of charge at a specific temperature (Q_exp_T, SoC_T).
4. **Pulse test & EIS** - Pulse tests and Electrochemical Impedance Spectroscopy tests, performed at three different SoC_T (20%, 50% and 80%).
5. **Temperature (optional)** - Repetition of sections 2, 3 and 4 at different temperatures (5°C, 25°C and 40°C).

Sections 1 serves as a "warm-up" of the cell, Sections 2 to 4 are the main characterization sections performed at 25°C or ambient temperature, which can be applied in sequence or independently, while Section 5 consists in the repetition of sections 2 to 4 in different thermal conditions. Being Section 2 and Section 5 the most time consuming, they are indicated as optional, which is, to be applied for extensive testing only.

The procedure takes as a reference the nominal technical specifications of a healthy cell, which can be obtained from either a commercial datasheet, or expected performance given the materials and geometry of in-house

Funded by the European Union
Views and opinions expressed are those of the author(s) only and do not necessarily reflect those of the European Union or CINEA. Neither the European Union nor the granting authority can be held responsible for them. This project has received funding from Horizon Europe research and innovation programme under Grant Agreement No.1069890

manufactured cells. The parameters set to perform each test, such as voltage thresholds, c-rates, temperature limits, etc. are then calculated from nominal specifications, values recorded along the same test, and predefined values.

3.2 Preliminary Work and Setup

3.2.1 Modules Disassembly

FBK received 1 module with 30 cells coming from the unpacking of a Hyunday Kona battery pack performed by ACCUREC, 4 cells coming from a module of the same type dismantled by CARTIF, and 4 Modules from a batch of batteries coming from Light Means of Transport (LMT) vehicles. All the received modules have been disassembled and dismantled into single cells. The information obtained during the disassembly process is contained in Table 3.1, while Figure 3.2 shows some pictures of the LMT modules and their disassembly.

***Table 3.1** - List of modules disassembled by FBK*

Name / Code	Specifications	Electrical Configuration	Cell Type	Status
HKO E P04 M01	36V, 180Ah	3p10s	Pouch	Good shape Cells voltages: [3.5-3.6V]
HKO E P05 M05 C01-04	3.6V, 60Ah	Single cells	Pouch	Good shape Cells voltages: [3.5-3.6V]
LMT L P01 M01	36V, 14Ah (calculated from cell specs)	1p10s	Prismatic	Good shape, 1 damaged cell Cells voltages: [3.55-3.56V]
LMT L P01 M02	25.2V, 14Ah	2p7s	Pouch	Some swollen cells Cells voltages: [0.8-1.2V]
LMT L P01 M03	36V, 10Ah	4p10s	Cylindrical	Good shape, Cells voltages: [3.70-3.71V]
LMT L P01 M04	Not available	Not clear	Cylindrical	Already unpacked Cells voltages: [2.7-3.6V]

Funded by the European Union

Views and opinions expressed are those of the author(s) only and do not necessarily reflect those of the European Union or CINEA. Neither the European Union nor the granting authority can be held responsible for them. This project has received funding from Horizon Europe research and innovation programme under Grant Agreement No.1069890

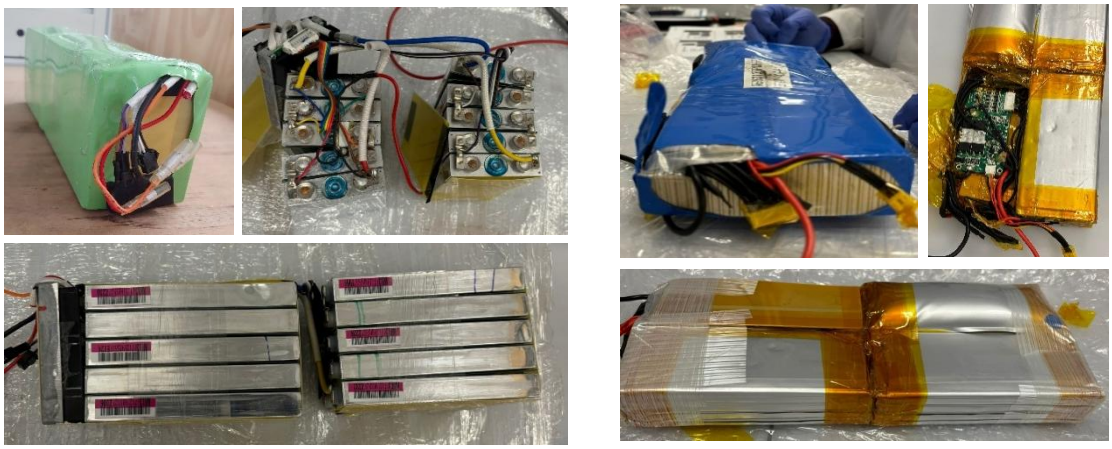

LMT L P01 M01 LMT L P01 M02

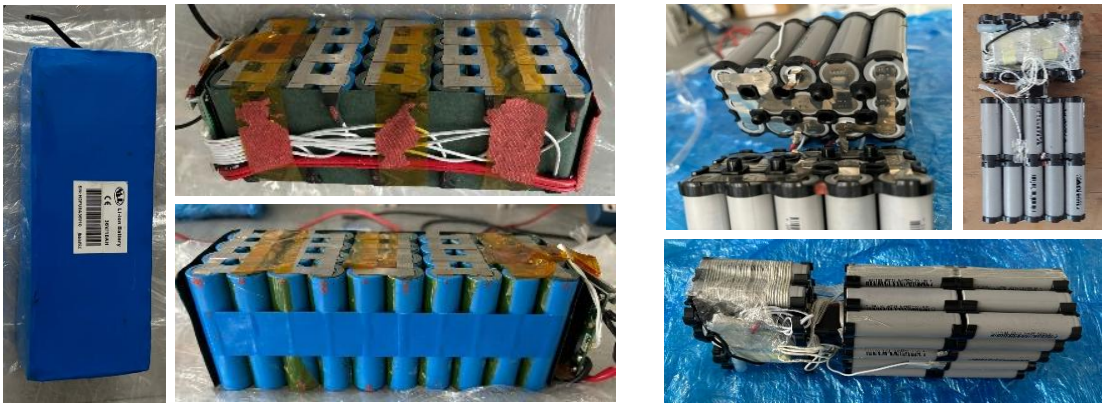

LMT L P01 M03 LMT L P01 M04

***Figure 3.1** · Pictures of the LMT modules along their disassembly*

Funded by the European Union

Views and opinions expressed are those of the author(s) only and do not necessarily reflect those of the European Union or CINEA. Neither the European Union nor the granting authority can be held responsible for them. This project has received funding from Horizon Europe research and innovation programme under Grant Agreement No.1069890

3.2.2 Cell Dismantling

A cell from the disassembled module was dismantled under a fume hood to understand the internal structure and obtain important information on the geometric parameters of the cell. These parameters will be used to build the models in T2.3. The cell HKO E P04 M01 C12 was selected for this task. This cell comes form a Hyundai Kona vehicle and its model is model is LG Chem E60B, featuring 60Ah capacity with NMC622 chemistry. First, the cell has been deep discharged in a controlled environment, then, to avoid safety issues connected to any residual energy content, it has been short-circuited for more than 10 hours.

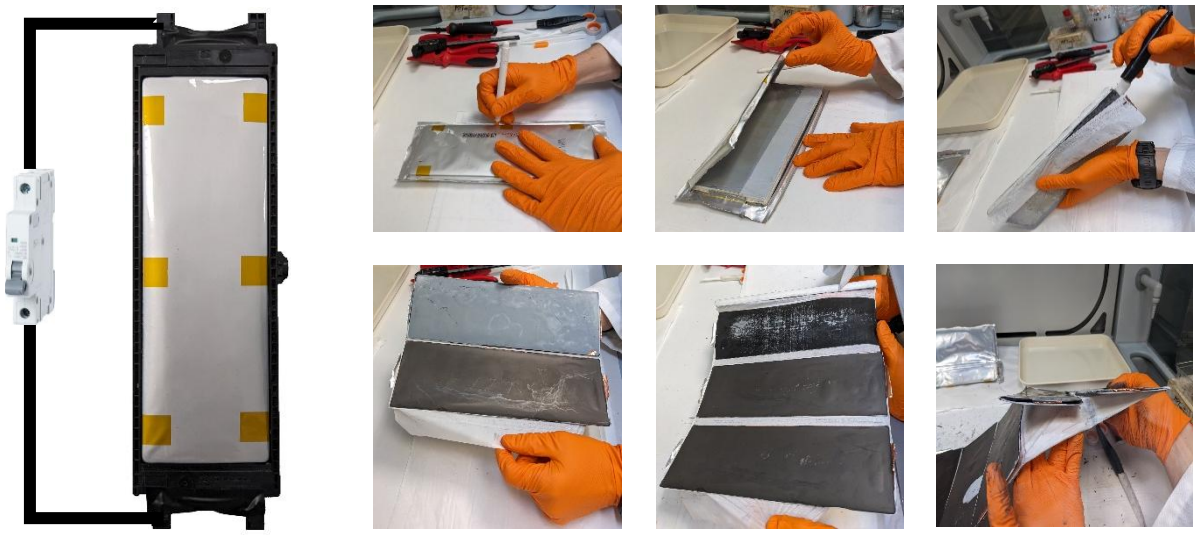

***Figure 3.2** · Pictures of the dismantling process of the cell HKO E P04 M01 C12*

Some pictures of the dismantling process are shown in Figure 3.2. The cell was opened under a fume hood using electrically resistive tools, such as plastic pincers and ceramic blades. The dismantled cell, unlike cells from other battery packs of the same model, showed yellow tapes on the external aluminium pouch. The observed internal structure is depicted in Figure 3.3.

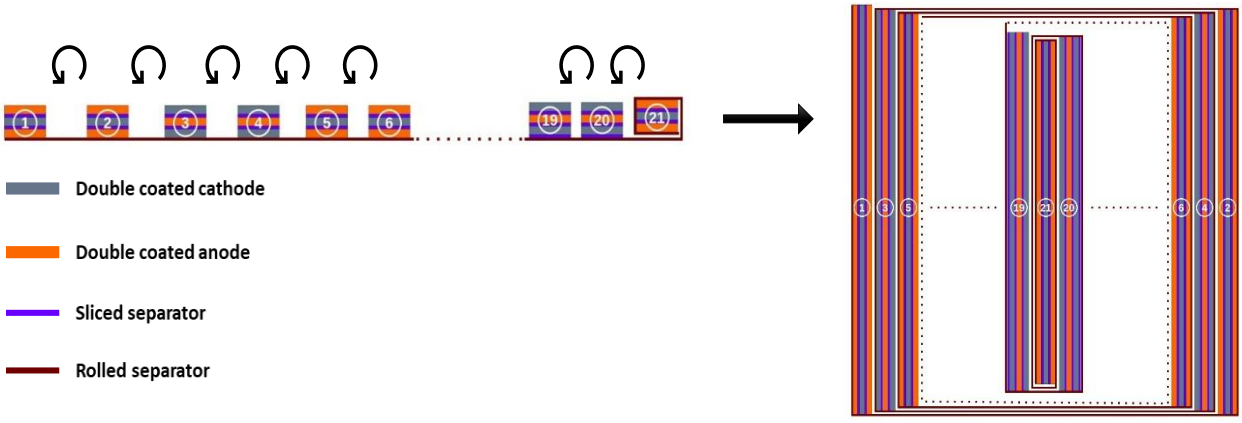

Figure 3.3 · Internal structure of the cell HKO E P04 M01 C12

Funded by the European Union

Views and opinions expressed are those of the author(s) only and do not necessarily reflect those of the European Union or CINEA. Neither the European Union nor the granting authority can be held responsible for them. This project has received funding from Horizon Europe research and innovation programme under Grant Agreement No.1069890

The construction of the cell features a rolled base separator with 21 set of electrodes. Each set of electrodes has either two negative and one positive electrodes or two positive and one negative electrodes. In addition, sliced separators are placed between each pair of positive and negative electrodes. Globally, the cell contains 32 double-coated anodes and 31 double-coated cathodes. Therefore, 63 double-coated electrodes in total (21 sets x 3), which result in 62 stacked cells. A rough measurement of electrodes thickness (current collector + 2 electrodes) performed with a plastic calliper shows 230 µm for the negative electrodes and 180 µm for the positive electrode.

3.2.3 Setup and Tests Summary

In the context of Task T2.2, several cells have been tested by FBK, with the aim to obtain complete characterizations and perform an analysis of their behaviour. All these cells have been tested inside an explosion proof thermal chamber Sanwood SMC-150-CB-FB, featuring an automatic fire extinguishing system. This allowed the possibility of overnight testing of relatively large cells, like the ones coming from Hyundai Kona battery packs.

All electrical tests have been performed with a Biologic potentiostat SP-150e + FlexP0012, with a 0-12V potential range and maximum current 200A, also able to perform EIS measurements. Every cell has been mounted on a cell holder, specifically designed to recreate pressure constraints similar to the ones present in mounted modules. On the cell, two thermal sensors are placed: a PT100 thermal resistance, connected to the fire safety system of the thermal chamber, and a thermocouple connected to the Biologic potentiostat. The described setup is shown in Figure .4

For validation of the setup, a first test was performed on the cell HKO E P04 M01 C14 (LG Chem E60B, 60Ah, NMC622) with climate chamber operating at 25°C. The applied procedure was the following:

- Preconditioning
  - Charge (CC+CV) 18A (standard charge C-rate)
  - Discharge (CC) 12A
- Capacity Tests
  - Charge (CC+CV) 18A (standard charge C-rate)
  - EIS (100% SoC)
  - Discharge (CC) at different C-rates
  - EIS (near 0% SoC)

Funded by the European Union

Views and opinions expressed are those of the author(s) only and do not necessarily reflect those of the European Union or CINEA. Neither the European Union nor the granting authority can be held responsible for them. This project has received funding from Horizon Europe research and innovation programme under Grant Agreement No.1069890

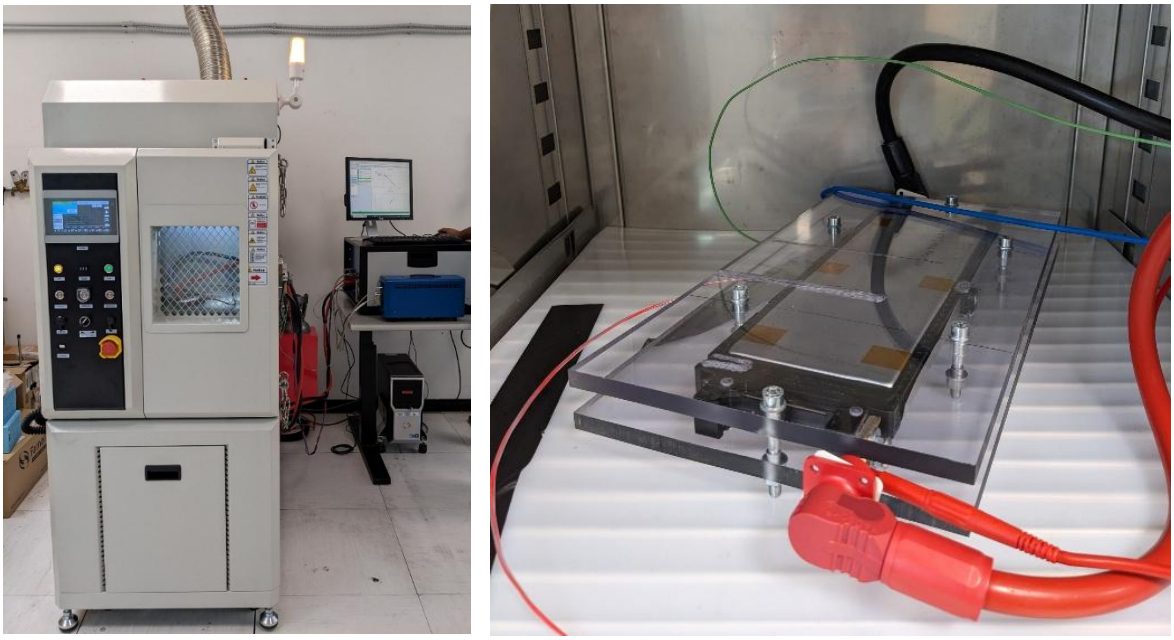

Figure 3.4 *· Setup for the electrochemical testing performed by FBK*

Results from the preliminary tests are shown in Figure 3.5. The cells discharge capacity showed to be between 56 and 60 Ah depending on C-rates. It must be noted that the cell temperature can increase significantly, even if the environment temperature is kept at 25°C. Specifically, it reached more than 40°C with the highest discharge rate of 1C. This effect is due to an excess of insulation, probably due to the thick walls of the cell holder. Observed temperatures were within 5°C to ambient temperature for C-rates of 0.5C or smaller.

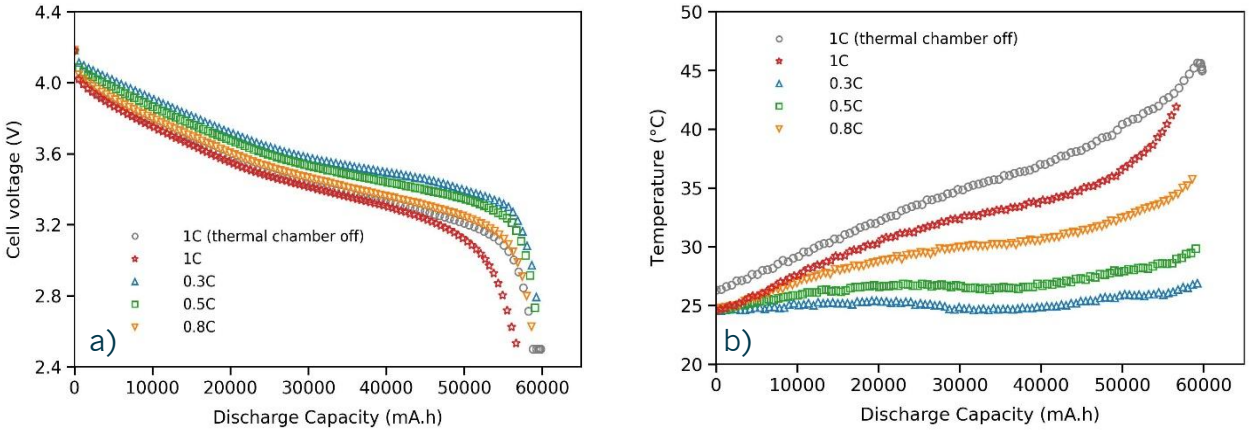

Figure 3.5 *· Preliminary tests for setup validation a) Cell Voltage vs Discharge Capacity; b) Cell Temperature vs DIscharge Capacity*

Funded by the European Union

Views and opinions expressed are those of the author(s) only and do not necessarily reflect those of the European Union or CINEA. Neither the European Union nor the granting authority can be held responsible for them. This project has received funding from Horizon Europe research and innovation programme under Grant Agreement No.1069890

Following the preliminary tests, two set of tests were performed on different cells. The first set includes full characterizations, performed applying the standard procedure described in the previous section. The second set, instead, investigates the behaviour of several cells under continuous cycling conditions at different C-rates and temperatures.

3.3 Cell Testing (Standard Procedure)

The testing with Standard Procedure was applied to 4 pouch cells of the type LG Chem E60B (60Ah, NMC622), namely HKO E P04 M01 C13&C14 (yellow taped) and HKO E P05 M05 C01&C04 (pink taped). Since all the cells were in a good shape and showed similar results, here only the results from cell HKO E P05 M05 C04 are shown. This cell was between the ones received from CARTIF and showed pink tapes on the external aluminium pouch. In any case, the electrochemical behaviour of pink taped and yellow taped cells did not show any substantial difference. On this cell, the standard procedure was repeated at three different temperatures. The summary of these tests are shown in Table 3.2.

***Table 3.2** - Tests performed on cell HKO E P04 M01 C14*

Tests	25°C	5°C	40°C
Preconditioning	x	-	-
Open Circuit Voltage	x	x	x
Energy and Capacity	x	x	x
Pules & IES	x	x	x

3.3.1 Tests at standard temperature (T=25°C)

As a first step of the procedure, a preconditioning was performed in thermal chamber at 25°C, applying two cycles at moderate current (12A, 0.2C). Following, the OCV section was applied, with a 3A charge (0.05C) and a 3A discharge (0.05C). Experimental data versus time is shown in ***Figure** 4*.6a.

Funded by the European Union

Views and opinions expressed are those of the author(s) only and do not necessarily reflect those of the European Union or CINEA. Neither the European Union nor the granting authority can be held responsible for them. This project has received funding from Horizon Europe research and innovation programme under Grant Agreement No.1069890

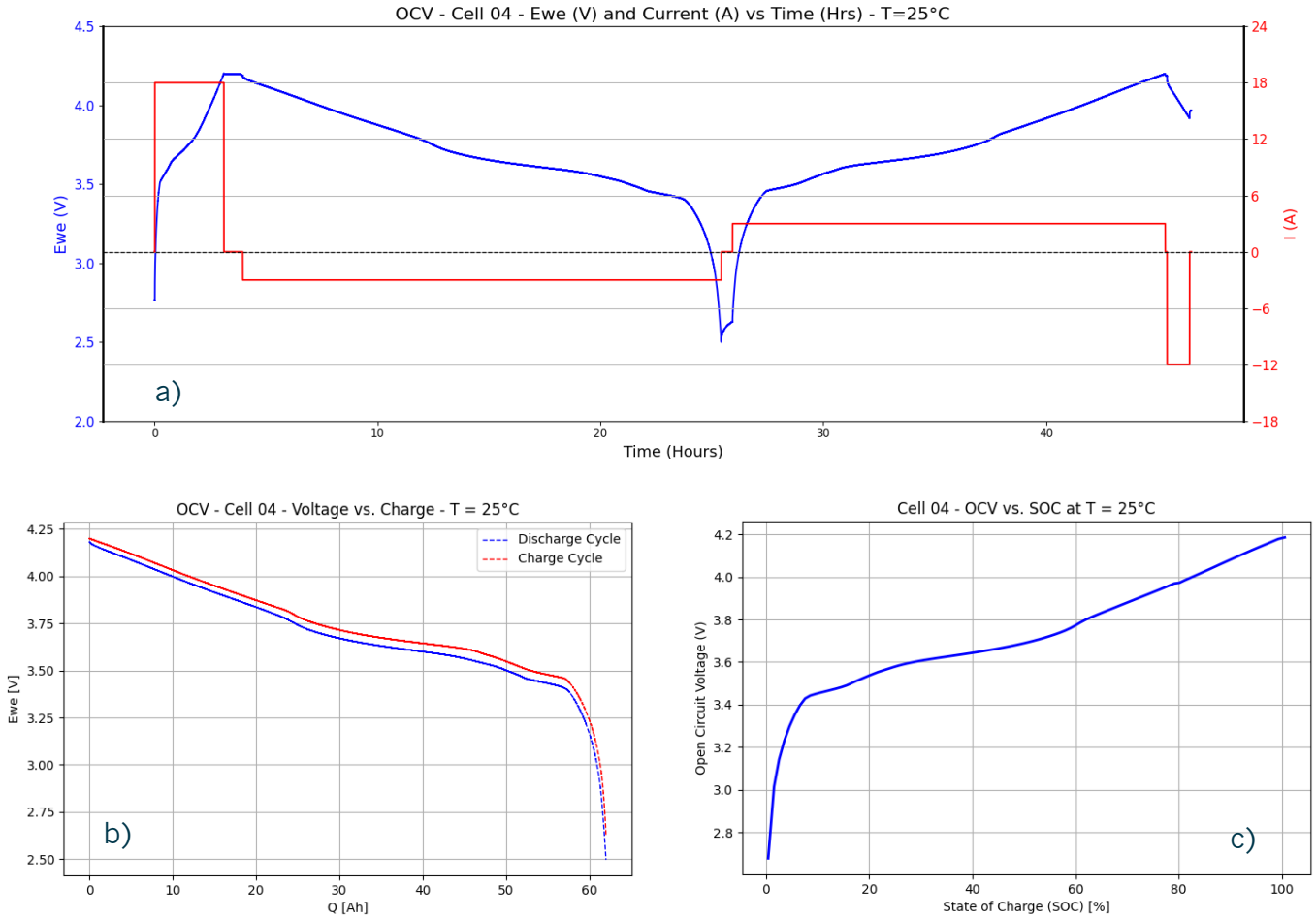

***Figure** 4.6 - Open Circuit Voltage Test - 3A charge (0.05C), 3A discharge (0.05C), T=25°C*

From the OCV section, it was possible to obtain Voltage vs Capacity curves (Figure 4.6b) and the OCV vs SoC curve (Figure 4.6c), by performing the average between charge and discharge voltage at the same capacity

$$OCV = \frac{V_{cha} + V_{dch}}{2}$$

and applying the following formula for the calculation of the SoC

$$SoC = 1 - \frac{Q}{Q_N}$$

where Q_N is the nominal capacity, equal to 60Ah.

After OCV, the Energy & Capacity section was performed, applying a standard 18A charge (0.3C) and discharging at 20A, 30A and 60A, (C/3, C/2 and 1C) for two cycles per C-rate. Experimental data versus time is shown in Figure .

Funded by the European Union

Views and opinions expressed are those of the author(s) only and do not necessarily reflect those of the European Union or CINEA. Neither the European Union nor the granting authority can be held responsible for them. This project has received funding from Horizon Europe research and innovation programme under Grant Agreement No.1069890

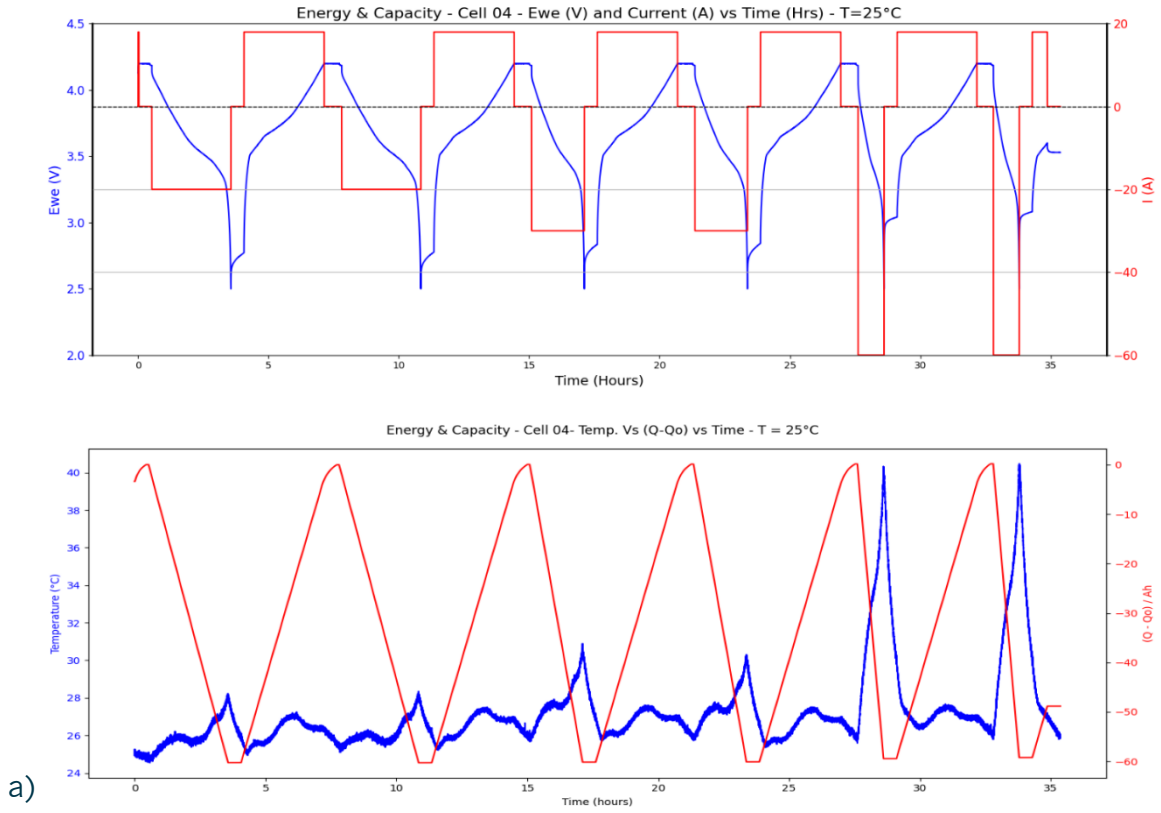

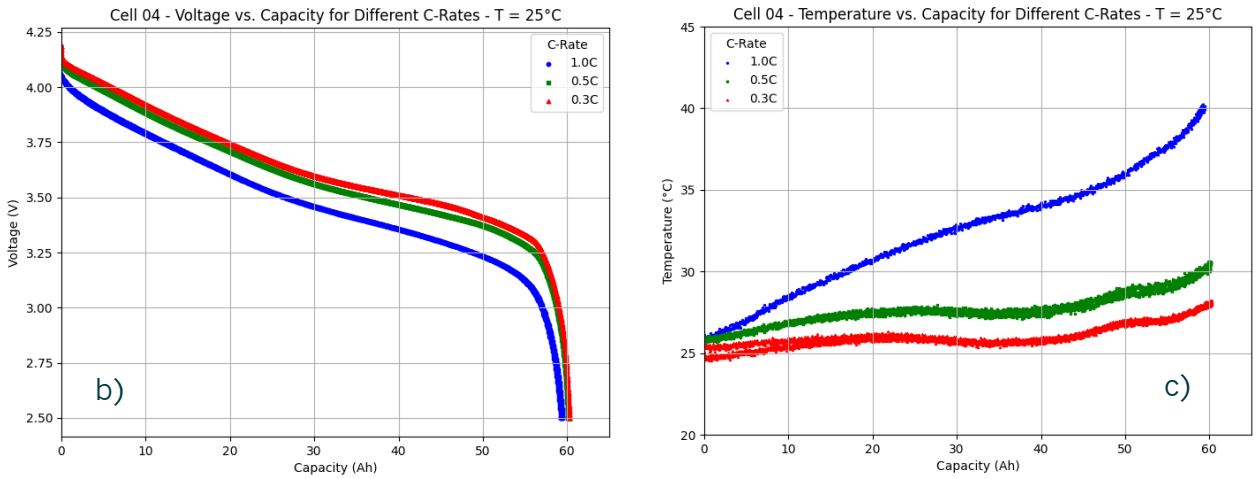

Figure 3.7 - *Energy and Capacity Test - 18A charge (0.3C), 20A,30A, 60A discharge (C/3, C/2, 1C), T=25°C*

Postprocessing on the second cycle for each C-rate allowed to obtain the Voltage vs Charge curve for different C-rates and the corresponding temperature behaviour of the cell. It must be noted that for each C-rate the cell reached an experimental capacity very close to the nominal one (60Ah), therefore showing very good State of Health (SoH). As expected, a higher overpotential (around 150 mV) is seen for the 1C discharge case, due to the

Funded by the European Union

Views and opinions expressed are those of the author(s) only and do not necessarily reflect those of the European Union or CINEA. Neither the European Union nor the granting authority can be held responsible for them. This project has received funding from Horizon Europe research and innovation programme under Grant Agreement No.1069890

high current. It must also be noted that, while the discharge temperature remained within 5°C with respect to the ambient one in the C/3 and C/2 cases, it steadily raised up to 40°C in the 1C case. This can be correlated with the increasing overpotential shown in the Voltage vs Capacity curve at decreasing SoCs.

As last step, the Pulse & EIS section was applied, performing subsequent Pulses and Potentiostatic EIS at 80%, 50% and 20% SoC. Time-dependent results are shown in Figure 3.8. At each SoC, the procedure applied three discharge pulses lasting 10s at 60, 120A and 180A (1C, 2C and 3C), each one followed by a charging pulse of variable duration to return to the original SoC. No significant differences were observed between the different SoCs in the voltage response to the pulse.

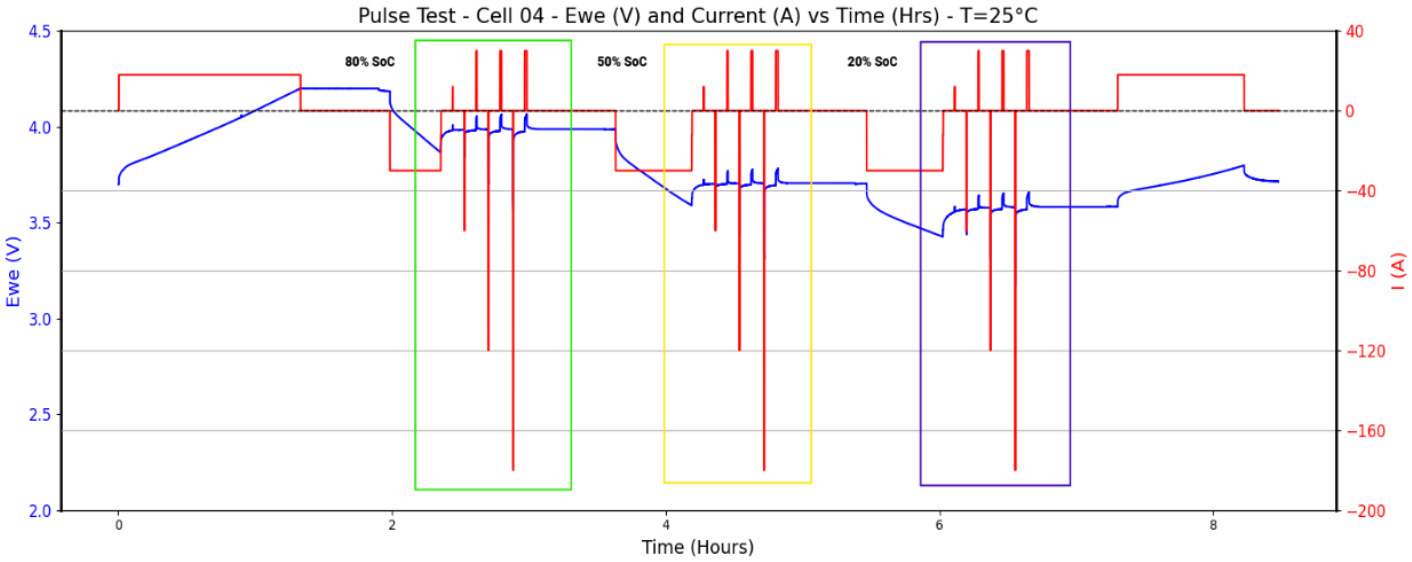

***Figure 3.8** · Pulse Test – 10s discharge pulses at increasing C-rates, T=25°C*

For each SoC, a PEIS was also applied with 10mV excitation with a [1mHz-100kHz] range. A Nyquist plot showing the impedance response of the cell at different State of Charge (SoC) levels is shown in Figure 3.9.

Funded by the European Union

Views and opinions expressed are those of the author(s) only and do not necessarily reflect those of the European Union or CINEA. Neither the European Union nor the granting authority can be held responsible for them. This project has received funding from Horizon Europe research and innovation programme under Grant Agreement No.1069890

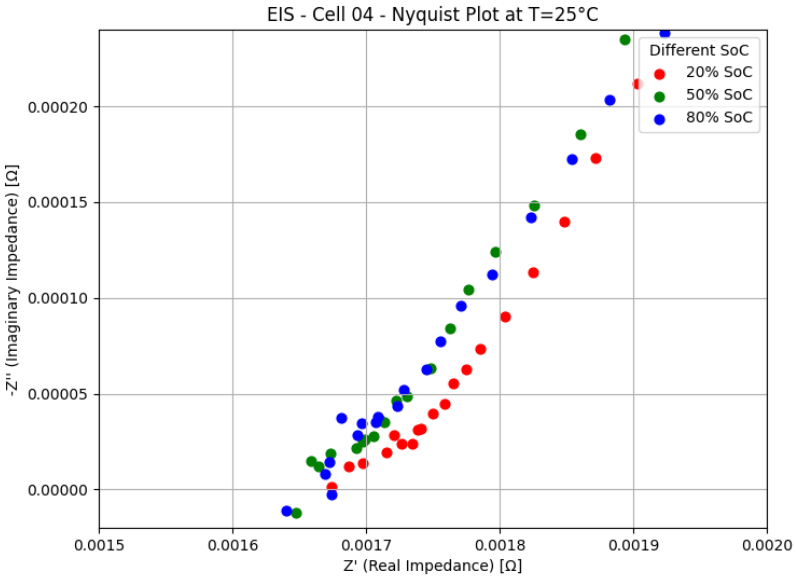

Figure 3.9 - *EIS Test – 10mV excitation at different SoCs, T=25°C*

3.3.2 Comparison Between Different Temperatures

The standard procedure has been applied at three different temperature to the same cell, namely 5°C, 25°C and 40°C. This section presents the comparison of the results of the different tests, after some elaboration steps. Figure shows OCV vs SoC obtained at the different temperatures, calculated as for previously explained equations.

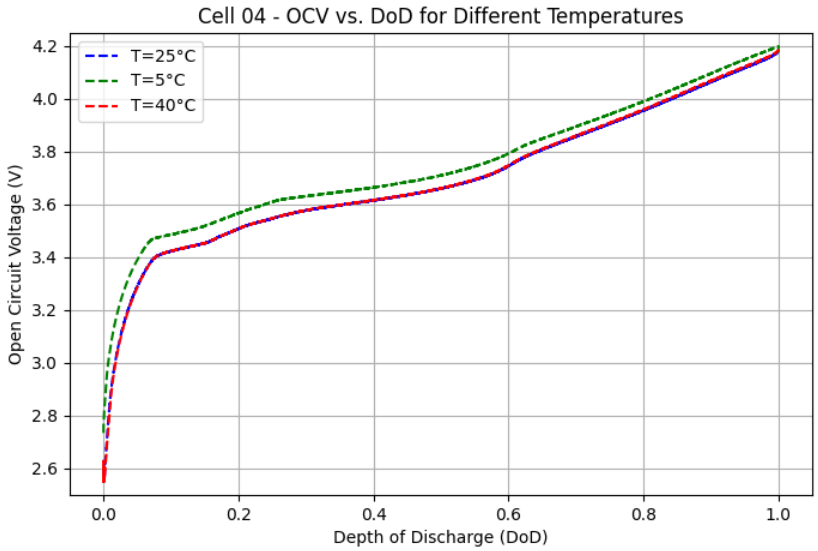

Figure 3.10*- Comparison of OCV vs SoC curves at different temperatures*

Funded by the European Union

Views and opinions expressed are those of the author(s) only and do not necessarily reflect those of the European Union or CINEA. Neither the European Union nor the granting authority can be held responsible for them. This project has received funding from Horizon Europe research and innovation programme under Grant Agreement No.1069890

The three curves follow the same pattern, with a slight higher voltage for the 5°C case. This can be due to the fact that the point identifying the 100% SoC is set at OCV equal to 4.2V, but at a different temperature for each test. A direct consequence is that the electrochemical status of the cell at 100% SoC is different for each test.

The results of Energy and Capacity section are shown in Figure 3.11. Here Voltage vs Capacity curves are compared at different temperatures for the same C-rate. Discharge at 1C at 40°C was skipped because the test was expected to exit from the thermal safety range of the cell [-20; 60°C]. Results clearly shows that the cell behaviour is very similar at 25°C and 40°C, while both capacity and overpotentials worsen at 5°C, especially at the highest C-rate (1C). This is due to the strongly reduced mobility of lithium ions and slowing down of reaction kinetics at low temperatures. The same effects can be clearly

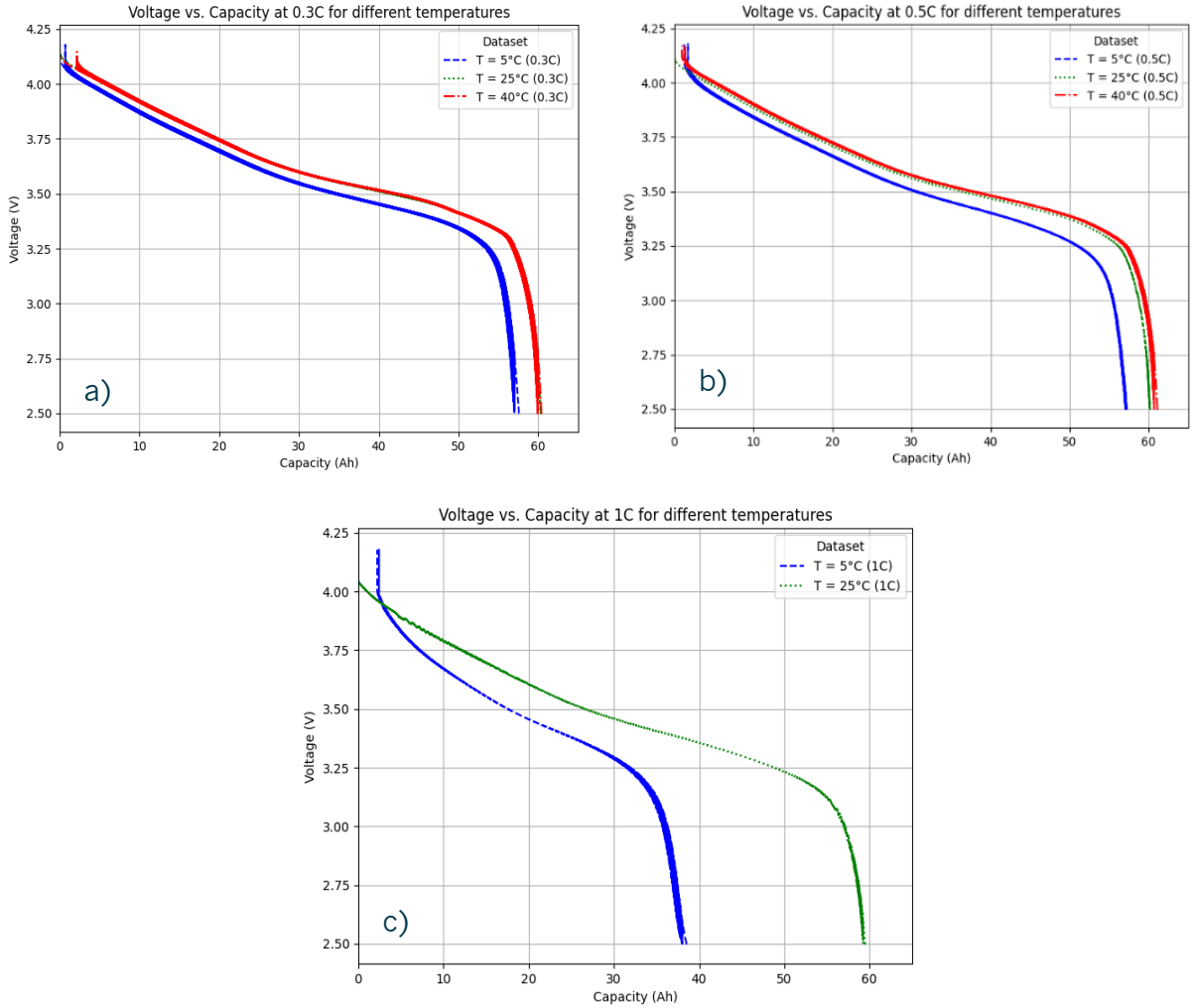

Figure 3.11 - *Cell Voltage vs Discharge Capacity at several temperatures for different C-rates: a) C-rate = 0.3C; b) C-rate = 0.5C; c) C-rate = 1C*

Funded by the European Union

Views and opinions expressed are those of the author(s) only and do not necessarily reflect those of the European Union or CINEA. Neither the European Union nor the granting authority can be held responsible for them. This project has received funding from Horizon Europe research and innovation programme under Grant Agreement No.1069890

seen in the EIS results in Figure 3.12. Ohmic resistance only slightly increases with decreasing temperatures, but charge transfer resistance changes of some orders of magnitude.

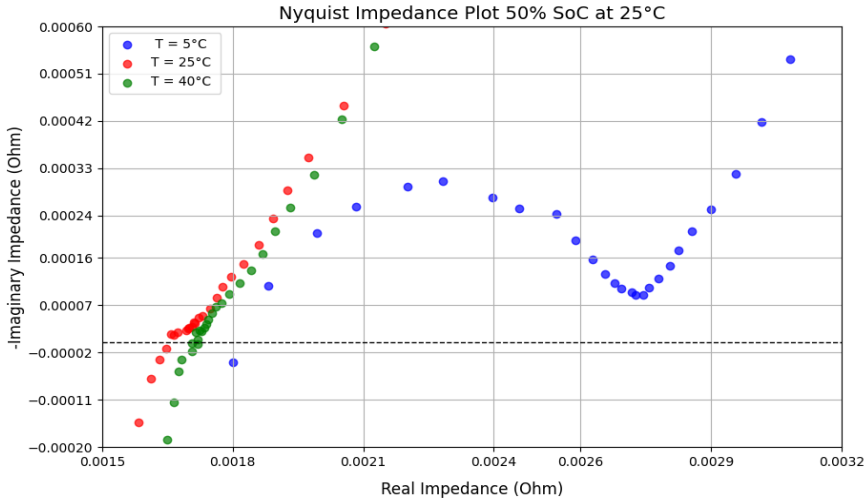

Figure 3.12 - *EIS Test at 50% SoC at different temperatures*

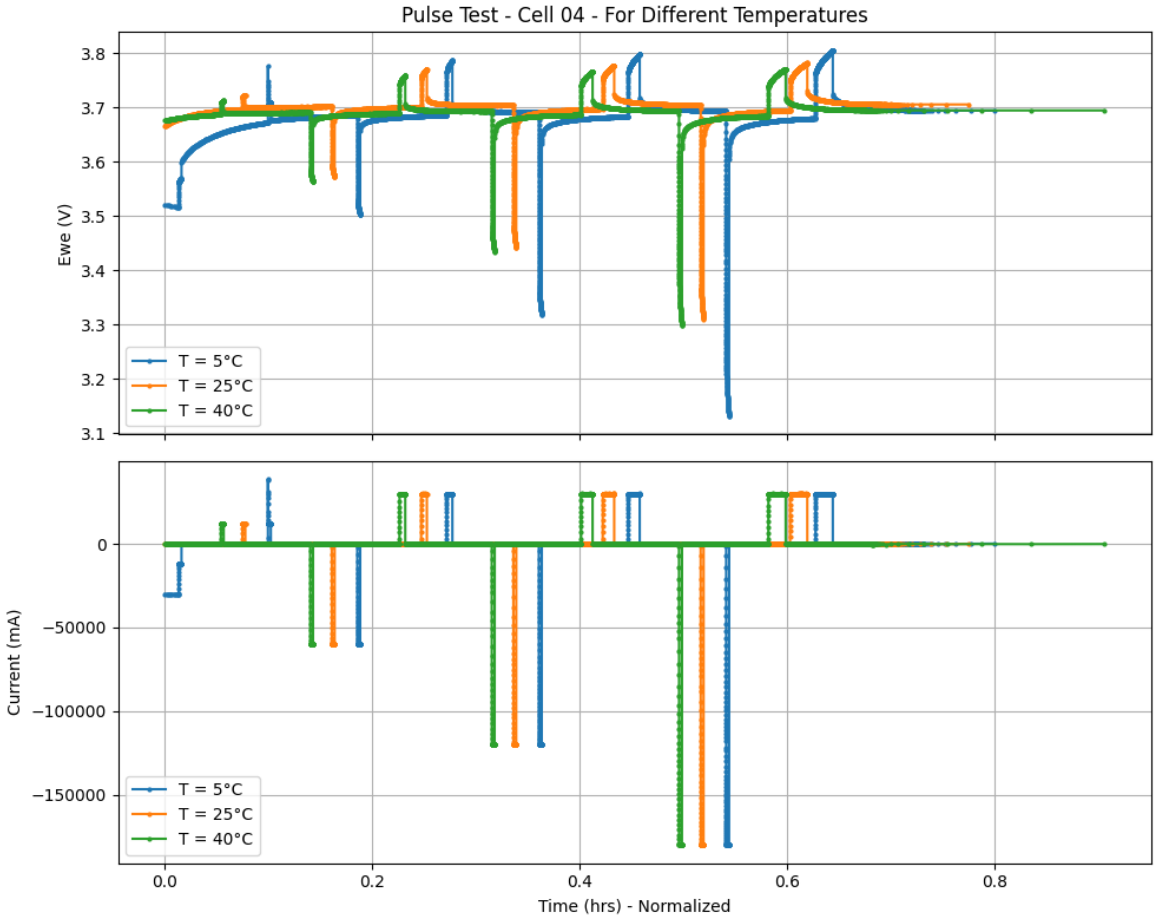

Figure 3.13 *- Pulse Test at 50% SoC at different temperatures*

Funded by the European Union

Views and opinions expressed are those of the author(s) only and do not necessarily reflect those of the European Union or CINEA. Neither the European Union nor the granting authority can be held responsible for them. This project has received funding from Horizon Europe research and innovation programme under Grant Agreement No.1069890

Pulse tests results, depicted in Figure 3.13, shows how the dynamic overpotential in discharge peaks is minimum at 25°c, slightly higher at 40°C, but considerably larger at 5°C. It is interesting to note that in charging pulses instead, the overpotential experienced at 40°C is substantially smaller than the one at 25°. This can be explained by the smaller currents used for charging pulses, which probably do not create a local heating as high as the very large peak currents used for discharging.

3.4 Cell Testing (Continuous Cycling)

To investigate the behaviour under intensive use, some cells have been tested applying a continuous cycling. These tests were performed at different C-rates and temperatures on two different cells, namely HKO E P04 M01 C13 and C14 (pouch cell, LG Chem E60B, 60Ah, NMC622).

3.4.1 Cycling Tests

Here follows the list of performed tests:

a. 18A charge (0.3C), 60A discharge (1C) at T = 25°C – Cell 14
b. 18A charge (0.3C), 20A discharge (C/3) at T = 25°C – Cell 13
c. 18A charge (0.3C), 20A discharge (C/3) at T = 37°C – Cell 13
d. 18A charge (0.3C), 60A discharge (1C) at T = 15°C – Cell 13
e. 18A charge (0.3C), 20A discharge (C/3) at T = 25°C – Cell 13 after 6 days resting

A resting period of 5 mins was applied between any charge and discharge phase and vice versa. Some tests stopped due to failure of the equipment or independent laboratory issues. Every time this happened, the test was restarted at the first suitable time within a couple of days.

Funded by the European Union

Views and opinions expressed are those of the author(s) only and do not necessarily reflect those of the European Union or CINEA. Neither the European Union nor the granting authority can be held responsible for them. This project has received funding from Horizon Europe research and innovation programme under Grant Agreement No.1069890

Figure 3.14 presents an extract of Test a. showing the pattern over time of voltage, current, temperature and charge capacity typical of the tests presented in this section.

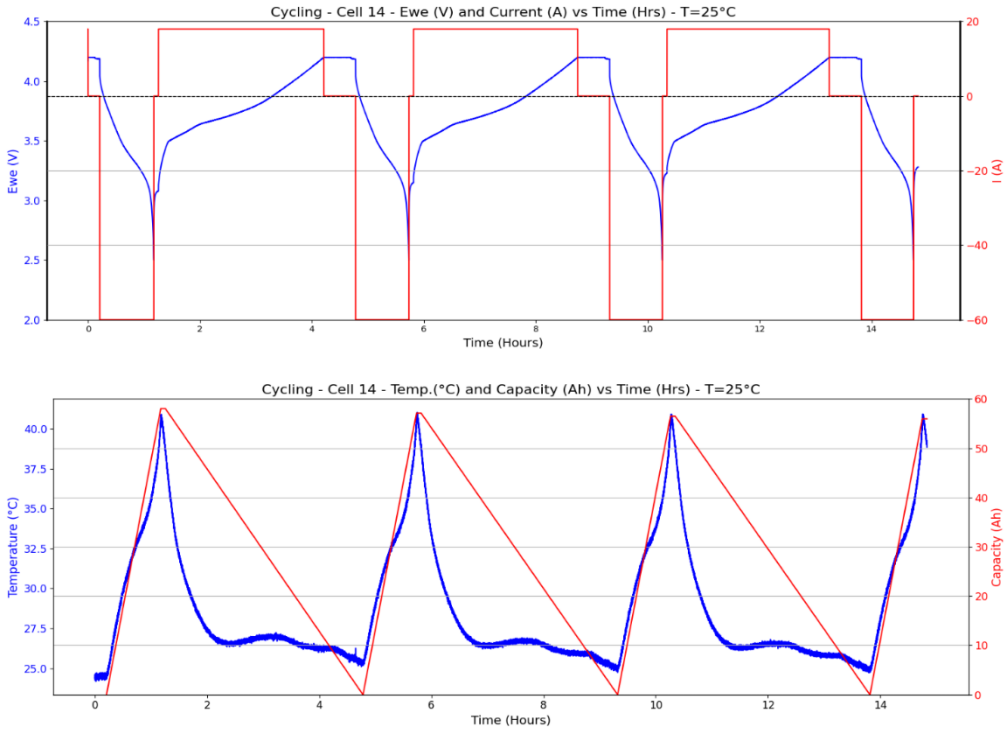

Figure 3.14 - *Extract of Test a. with 1C discharge at T=25°C*

The charge phase is performed in constant current + constant voltage mode (CC+CV), while the discharge phase is in constant current. Just 5 mins of rest is left between each phase, therefore not leaving much time for thermodynamic stabilization of the cell.

It must be noted that the temperature of the cell is not constant and it strongly depends on the applied C-rate. Generally, the cell temperature increases during the discharge, with the maximum value obtained at the end of this phase, as a consequence of the large heat dissipation associated with high currents. During the charging phase, the temperature generally decreases, since the internal heat generation is limited and the cell is cooled by external natural convection. This behaviour is predominant at high C-rates, while temperature oscillations due to entropic heat generation and absorption are prevailing at low C-rates and at the end of charging phases.

Funded by the European Union

Views and opinions expressed are those of the author(s) only and do not necessarily reflect those of the European Union or CINEA. Neither the European Union nor the granting authority can be held responsible for them. This project has received funding from Horizon Europe research and innovation programme under Grant Agreement No.1069890

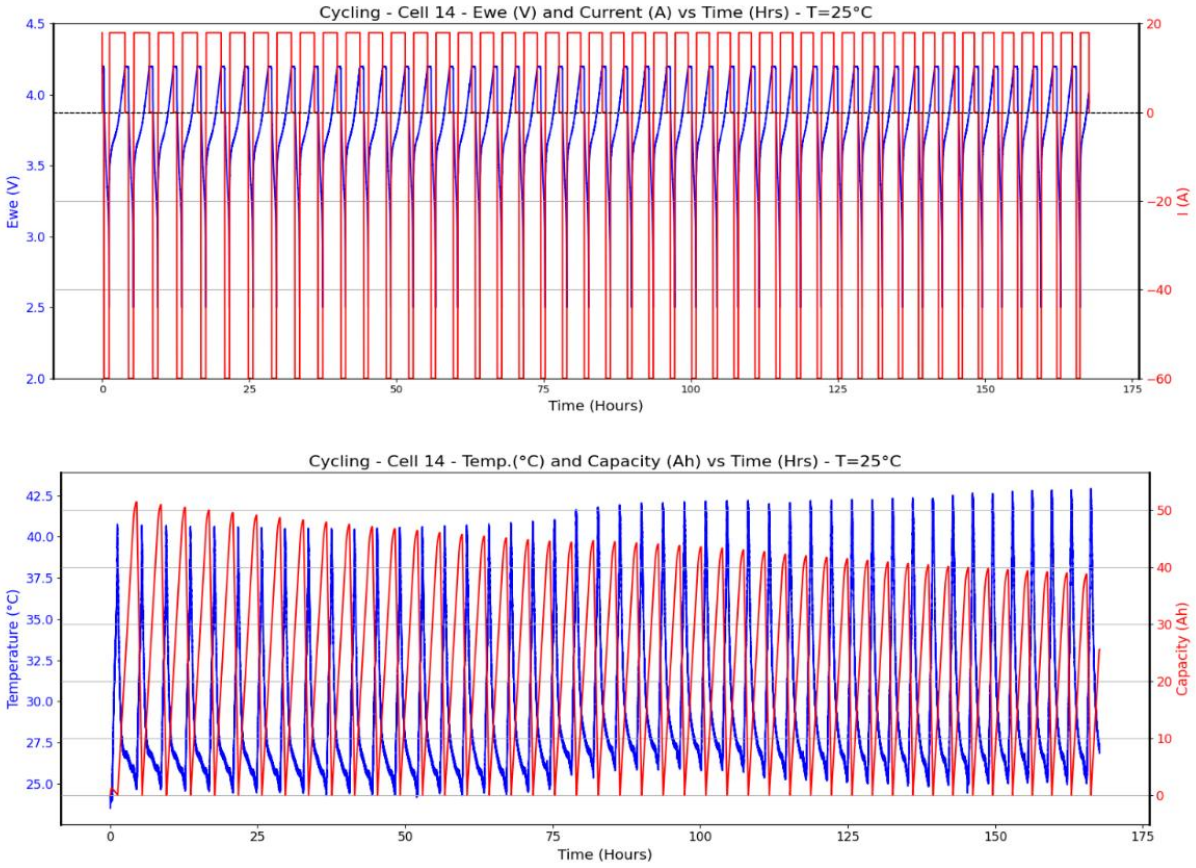

Figure 3.15 - *Test a. 18A charge (0.3C), 60A discharge (1C) T=25°C*

Time-dependent results from Test a. are shown in Figure while discharge capacity and maximum temperature per cycle are shown in Figure 3.16. Due to the fast discharging C-rate (1C), a large temperature oscillation is observed.

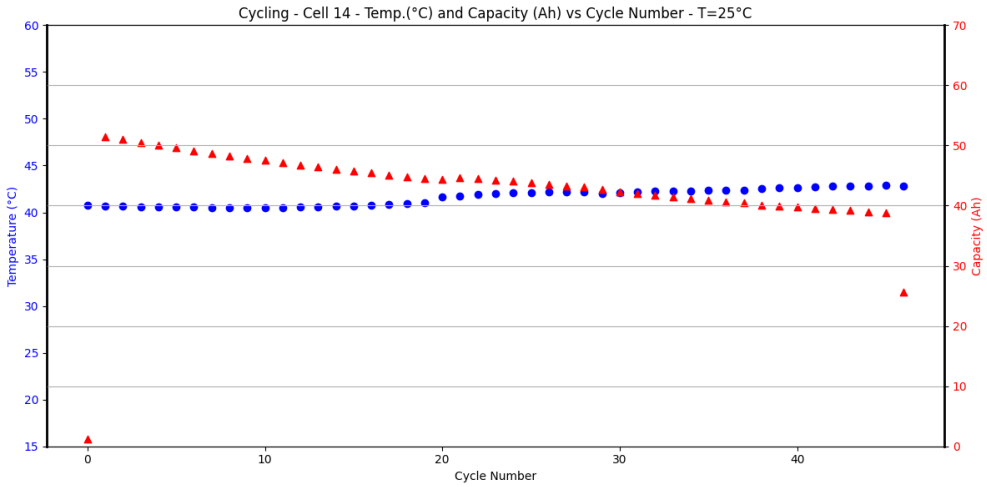

Figure 3.16 - *Test a. Maximum Temperature and Discharge Capacity vs Cycle Number*

Funded by the European Union

Views and opinions expressed are those of the author(s) only and do not necessarily reflect those of the European Union or CINEA. Neither the European Union nor the granting authority can be held responsible for them. This project has received funding from Horizon Europe research and innovation programme under Grant Agreement No.1069890

Its values increase over 40°C at the end of each cycle, to drop again around 25°C during the subsequent charging phase. The maximum temperature observed is 43°C.

A constant fade of the discharge capacity is clearly visible, with a total decrease of 25.6% in 46 cycles. The initial capacity of the cell was 52.2Ah, due to the fact that the same cell previously undergone some shorter preliminary cycling tests with the same procedure. Globally, this tests shows an average capacity fade of 0.56% per cycle.

To investigate the cause of the observed capacity fade, another test was set with a new cell (C13) at the same temperature, but a slower discharging C-rate of C/3. Time-dependent results of this test (Test b.) are shown in Figure , while discharge capacity and maximum temperature per cycle are shown in Figure 3.18.

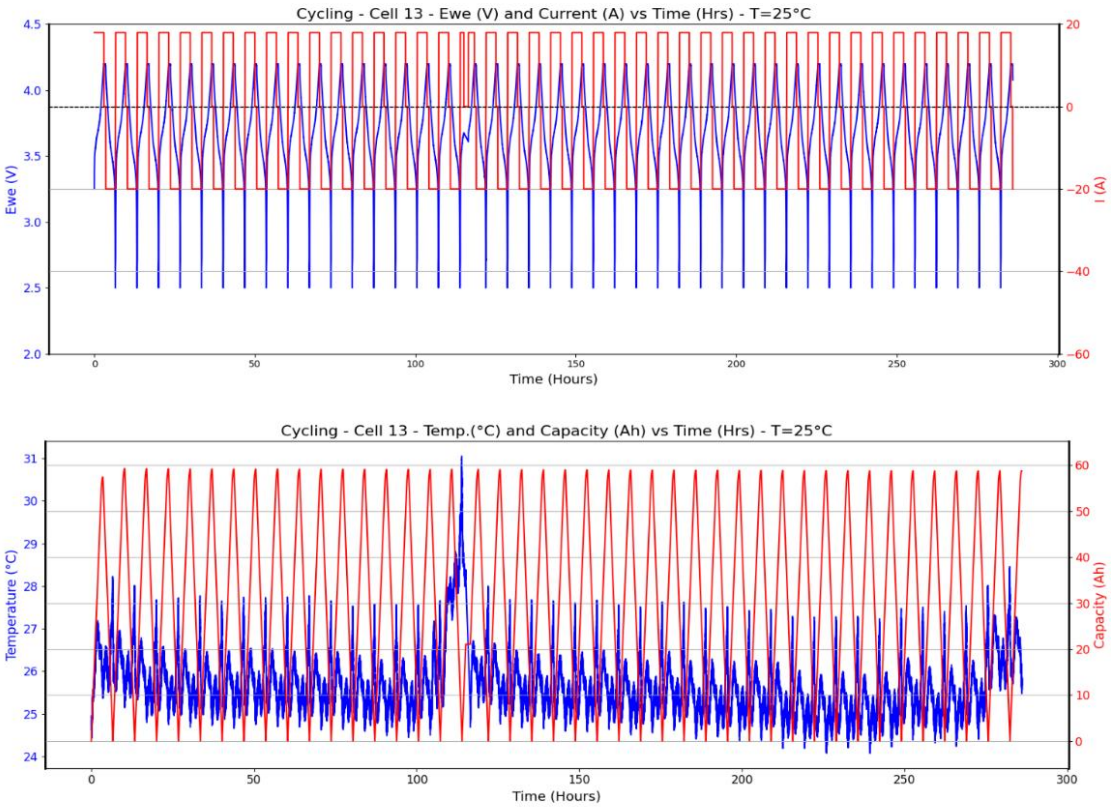

Figure 3.17 - *Test b. 18A charge (0.3C), 20A discharge (C/3) Tch=25°C*

This test showed very small temperature oscillations, registering values in average between 25°C and 28°C. The only exception is seen at cycle n. 16 and 17, due to a temporary standby of the thermal chamber. Even during this short period, the temperature remained below 32°C.

Funded by the European Union

Views and opinions expressed are those of the author(s) only and do not necessarily reflect those of the European Union or CINEA. Neither the European Union nor the granting authority can be held responsible for them. This project has received funding from Horizon Europe research and innovation programme under Grant Agreement No.1069890

This test showed almost no change in the discharge capacity, with 0.33% lost over 43 cycles. The average capacity fade was almost null, registering a 0.0076% per cycle.

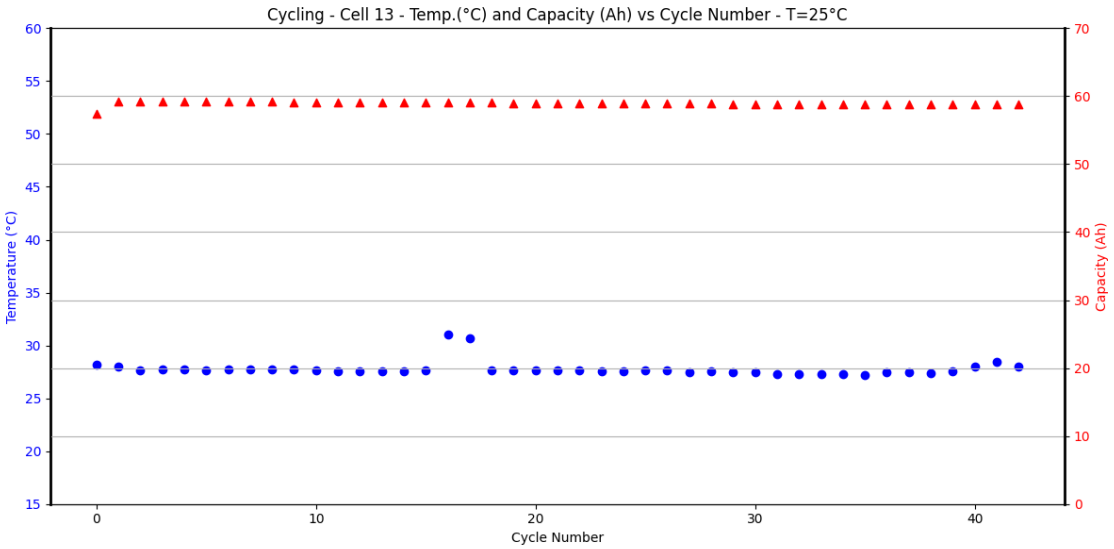

Figure 3.18 - *Test b. Maximum Temperature and Discharge Capacity vs Cycle Number*

Test b. demonstrated that the capacity fade in Test a. was due to the peculiar conditions of that test, that are high C-rates and high temperatures reached at the end of the discharge phases. To discriminate between the two effects, two more tests were performed, namely Test c., at high temperature and slow C-rate, and Test d., at low temperature and fast C-rate.

Time-dependent results of Test c. are shown in Figure , while discharge capacity and maximum temperature per cycle are shown in Figure .

Funded by the European Union

Views and opinions expressed are those of the author(s) only and do not necessarily reflect those of the European Union or CINEA. Neither the European Union nor the granting authority can be held responsible for them. This project has received funding from Horizon Europe research and innovation programme under Grant Agreement No.1069890

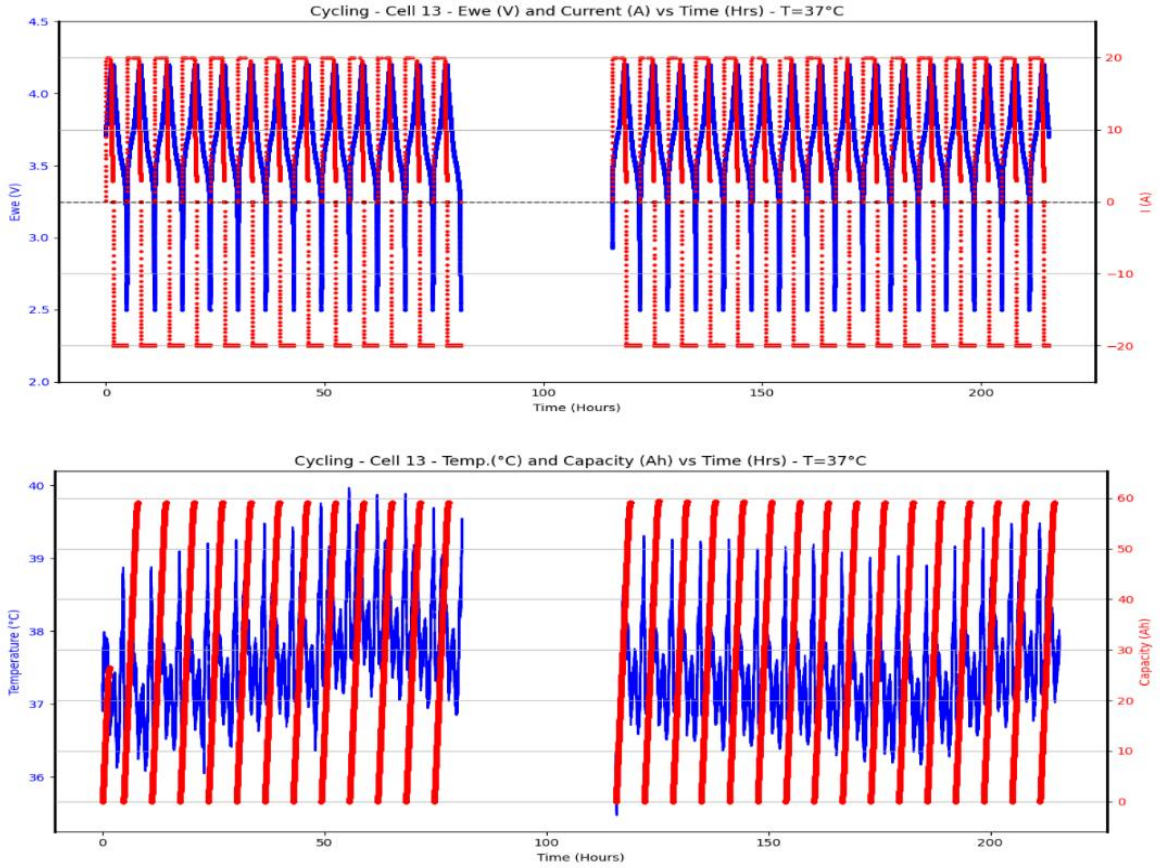

Figure 3.19- *Test c. 18A charge (0.3C), 20A discharge (C/3) Tch=37°C*

This test was unfortunately interrupted by a failure of the cycler, and restored after 36 hours, therefore the graphs in Figure 3.19 show an empty interval. This test showed small temperature variations, associated with low C-rates, with values mildly oscillating between 36°C and 40°C.

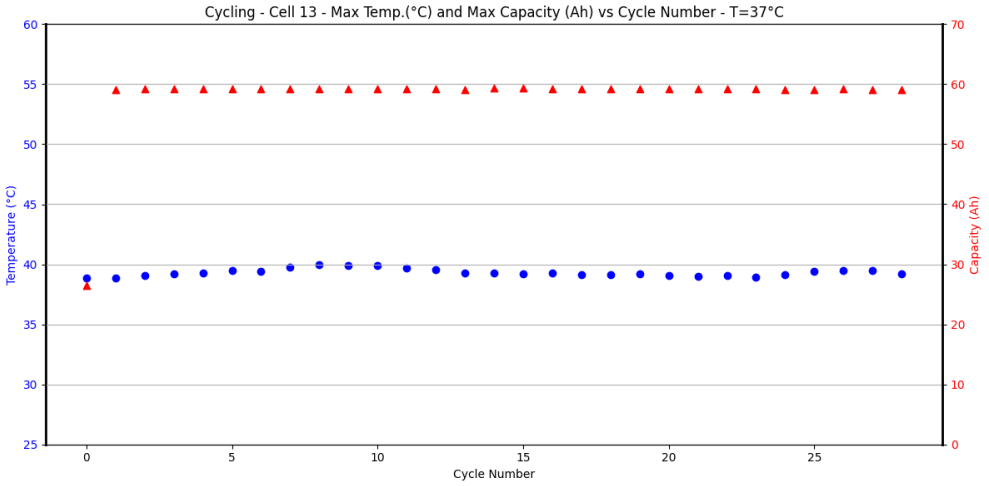

Figure 3.20 - *Test c. Maximum Temperature and Discharge Capacity vs Cycle Number*

Funded by the European Union

Views and opinions expressed are those of the author(s) only and do not necessarily reflect those of the European Union or CINEA. Neither the European Union nor the granting authority can be held responsible for them. This project has received funding from Horizon Europe research and innovation programme under Grant Agreement No.1069890

Discharge capacity also remained very stable, with a total loss of only 0.1% over 28 cycles. The average capacity fade results almost null at 0.0035% per cycle. This data demonstrates that the capacity loss observed in Test a. was not due to the high temperatures reached in the discharge phases. To further demonstrate this hypothesis, a last test (Test d.) was performed at low temperature and fast C-rates.

Time-dependent results of Test d. are shown in Figure 3.21, while discharge capacity and maximum temperature per cycle are shown in Figure .

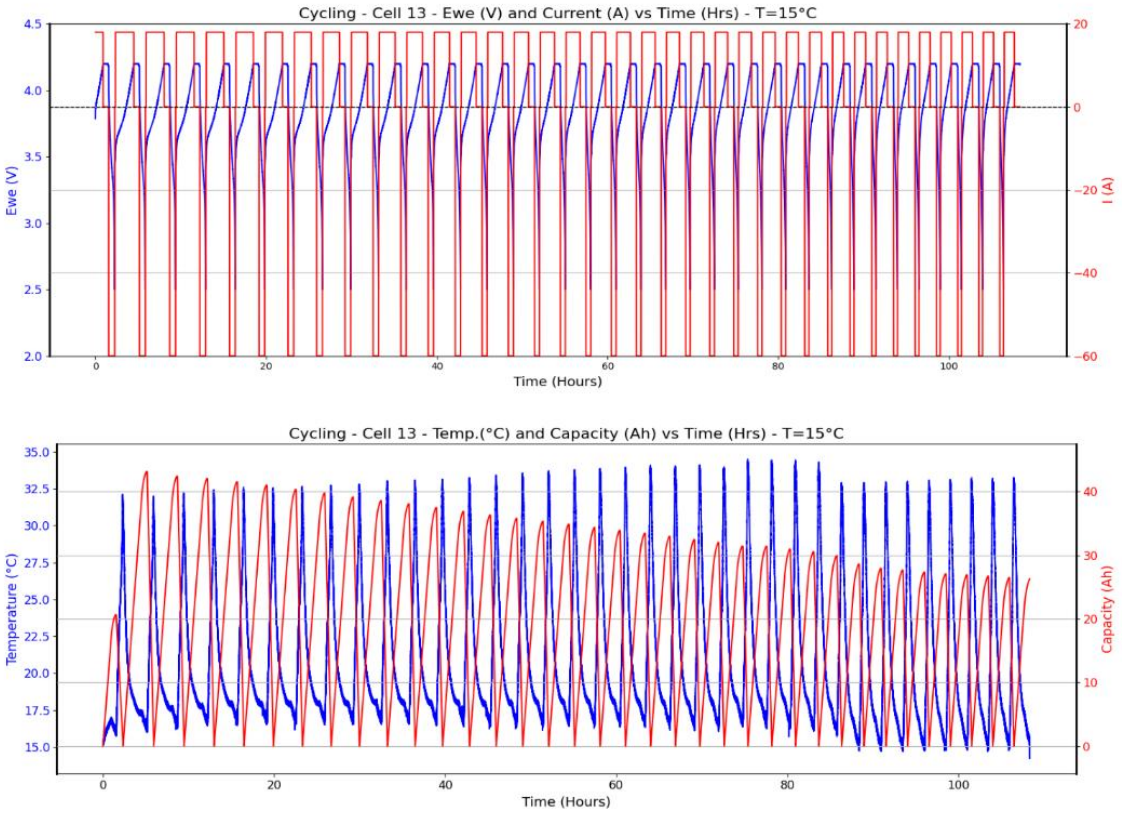

Figure 3.21 - *Test d. 18A charge (0.3C), 60A discharge (1C) Tch=15°C*

This test showed very large temperature oscillation, with very strong heating in the discharge phase, bringing the temperature from the 15°C baseline to values over 34°C. The combination of low environmental temperature and fast C-rate (1C), produced an even stronger heating effect. This effect is coherent with the larger overpotentials observed at low temperatures in the Standard Characterization, which would produce more irreversible heat generation.

Funded by the European Union

Views and opinions expressed are those of the author(s) only and do not necessarily reflect those of the European Union or CINEA. Neither the European Union nor the granting authority can be held responsible for them. This project has received funding from Horizon Europe research and innovation programme under Grant Agreement No.1069890

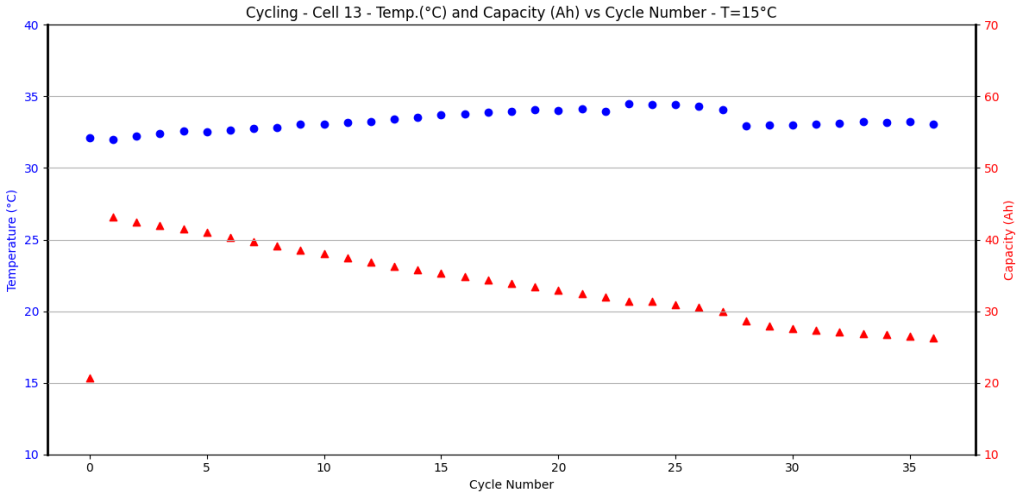

Figure 3.22 - *Test d. Maximum Temperature and Discharge Capacity vs Cycle*

Test d. showed a decrease in discharge capacity of 64.5% in 18 cycles, with an average capacity fade 3.5% per cycle. This demonstrate that the capacity loss is totally correlated with the large discharge C-rate, with even stronger effects at low temperatures.

After 6 days of rest, the same cell was tested again at 25°C and slow C-rate (C/3) in Test e., which results are shown in Figure . Unexpectedly, the cell

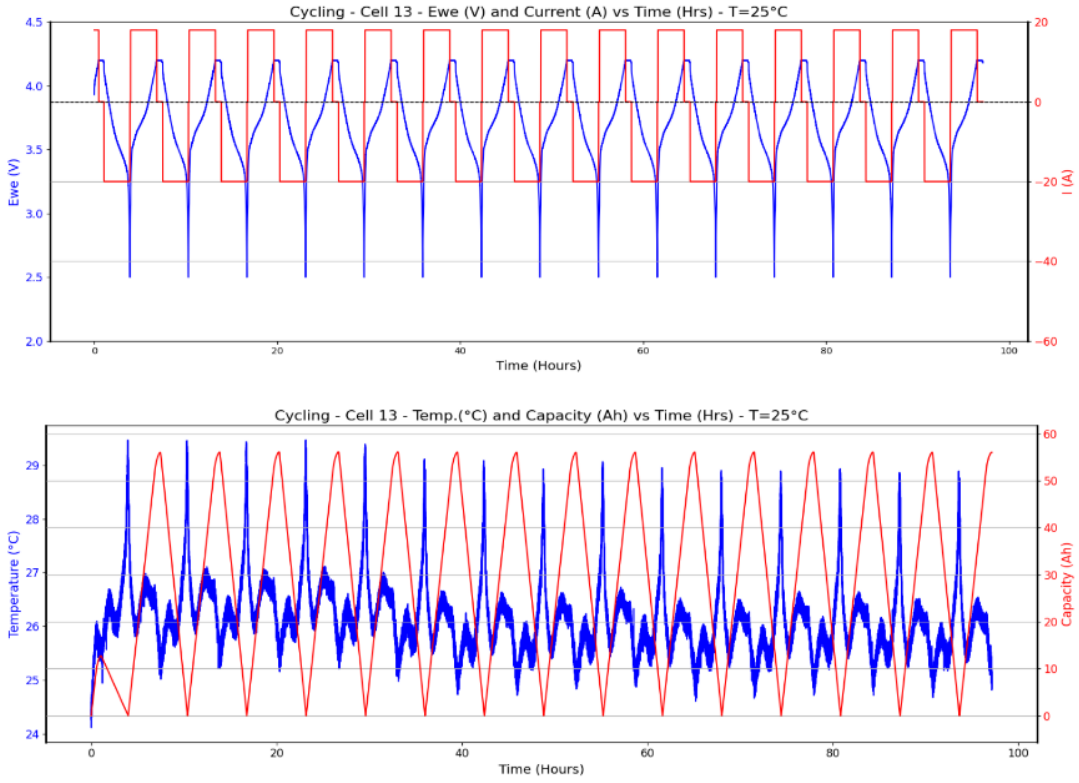

Figure 3.23 - *Test e. 18A charge (0.3C), 20A discharge (C/3) at T = 25°C*

Funded by the European Union

Views and opinions expressed are those of the author(s) only and do not necessarily reflect those of the European Union or CINEA. Neither the European Union nor the granting authority can be held responsible for them. This project has received funding from Horizon Europe research and innovation programme under Grant Agreement No.1069890

showed an almost complete recovery from the conditions reached at the end of Test d., with a stable capacity of 56.0 Ah. This correspond to the 94% of the original 59.5 Ah observed in Test b. at the same conditions. In comparison with the 35.5% remaining in the last cycle of Test d., it means recovering 90.7% of the lost capacity. This last test reveals that, probably, the short resting times between cycles also had an effect on the capacity fade.

3.4.2 Discussion and Conclusions

To further investigate on the cause of this decay, Pulse and EIS tests have been performed just after Test c., Test d. and Test e.. The ones after Test d. were performed at a SoC higher that 50% to avoid reaching the reduced capacity limit of the cell. Table 3 summarizes the data extracted by the Nyquist plot in Figure 3.24a.

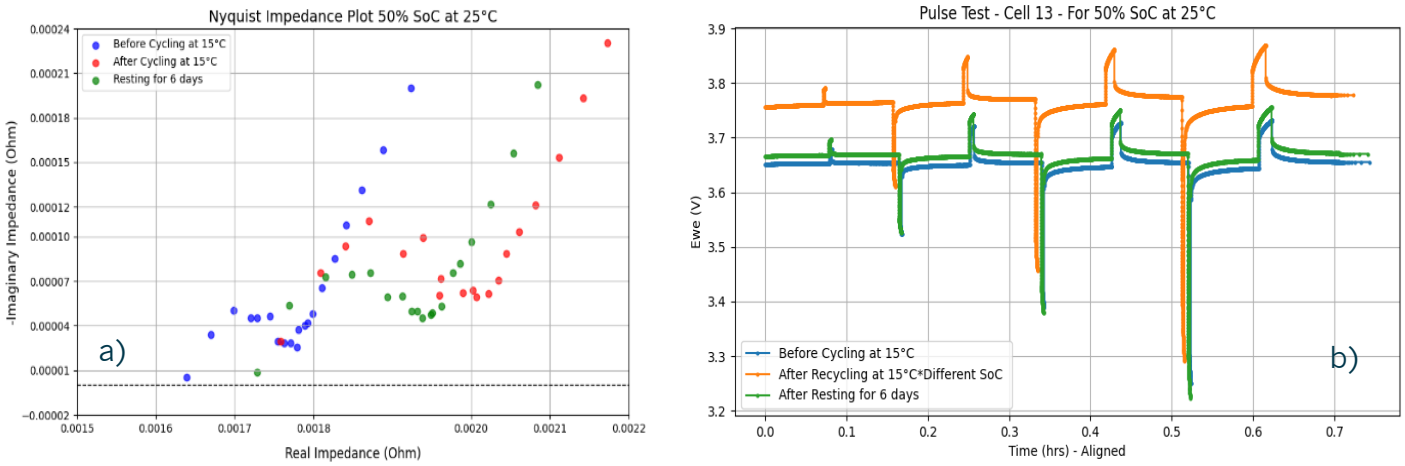

***Figure 3.24 – Tests** performed on Cell 13 after Test c., Test d. and Test e. a) EIS Test; b) Pulse Test*

***Table 3.3 –** Results extracted from EIS test on degradation of cell resistance*

EIS Test Time Position	Ohmic Resistance	Increase vs Test c.	Charge-Transfer Resistance	Increase vs Test c.
After Test c.	1.63 mΩ	-	0.15 mΩ	-
After Test d.	1.75 mΩ	7.3%	0.27 mΩ	80%
After Test e.	1.72 mΩ	5.5%	0.23 mΩ	53%

Results show that the ohmic resistance of the cell increased by 7.3% when cycling at 1C in 15°C environment (Test d.) and recovered 24% of this increase in the following 6 days. Similarly, the charge transfer resistance heavily

Funded by the European Union
Views and opinions expressed are those of the author(s) only and do not necessarily reflect those of the European Union or CINEA. Neither the European Union nor the granting authority can be held responsible for them. This project has received funding from Horizon Europe research and innovation programme under Grant Agreement No.1069890

increased by 80% after Test d., but recovered 34% of this increase during the resting period. This can be interpreted by supposing the degradation be caused mainly by microstructural changes in the electrodes, like particle cracking.

Data extracted from EIS tests confirm the self-healing behaviour. However, the internal resistance recovery shows a lower magnitude with respect to the one of discharge capacity. Pulse tests qualitatively confirm this behaviour. We can conclude that, in this type of cell, continuous cycling with high C-rates and short resting time leads to temporary capacity loss and partially irreversible decrease of the internal resistance.

These cells come from batteries of recalled vehicles of the Hyundai Kona type that were probably not used much, but still were affected by calendar aging. Aging can exacerbate the reversible capacity loss observed during cycling even at moderate C-rates. Aged cells have a larger internal resistance and this can enhance polarization effects. In addition, older cells may have more significant lithium plating issues, especially if they have been subjected to high C-rates or low temperatures during their lifetime. Finally, another important effect is related to structural degradation: the active materials can undergo structural changes over time such as particle cracking or loss of contact with the conductive matrix. These changes can increase polarization and reduce the efficiency of lithium-ion transport. The reversible nature of some of these effects during rest periods helps explain the temporary recovery of capacity observed during cycling.

As a continuation of this work, dismantling of aged cells and material characterizations could be used to directly observe possible morphological or chemical modification of the electrode surfaces. This would allow to distinguish between different aging mechanisms and identify which ones are associated with capacity recovery. In particular, optical and electron microscopy can be used to identify morphological and structural changes in the electrode, as well as presence of plated lithium. On the other hand, XPS can be employed to investigate the properties of the electrode surface and the chemical integrity of the solid-electrolyte interface.

Funded by the European Union

Views and opinions expressed are those of the author(s) only and do not necessarily reflect those of the European Union or CINEA. Neither the European Union nor the granting authority can be held responsible for them. This project has received funding from Horizon Europe research and innovation programme under Grant Agreement No.1069890

4. Electrochemical Characterization of EOL Cells (NESSTEC and SAU)

Within the scope of this task performed by NESSTEC and SAU, used lithium-ion batteries were collected from various sources and initially disassembled and classified as part of other WPs. Following this classification, electrochemical characterization was conducted to assess key parameters such as state of charge (SOC) and state of health (SOH). This section presents the first set of findings within this deliverable, focusing on the evaluation of used battery cells for their suitability in second-life applications. Additionally, cells deemed unsuitable for reuse were classified for recycling, contributing to the overall strategy for sustainable battery lifecycle management. As a note that the electrochemical tests in this section performed not based on the procedure given AnnexA due to lack of temperature chamber and some safety concern from damaged parts. Therefore, very limited short tests performed and presented in Figure 4.2.

Table 4.1. *Partner activities of the electrochemical characterization of spent cells (NESSTEC and SAU).*

Partner	Laboratory Status	Received Cells	Testing
SAKARYA	Overnight cell testing Ambient temperature	4 LMT modules (2 not damaged)	4 Cells Tested Std. (#5)
NESSTEC	Overnight cell testing Ambient temperature	4 LMT modules (2 not damaged)	4 Cells Tested Std. (#4)

Table 4.1 present the activities for responsible partners on electrochemical evaluation of spent cells. FBK, operating with a thermal chamber, received 34 cells in total (30 from one source and 4 from another, with 2 undamaged) and performed a combination of dismantling, standard, and aging tests on these cells. These results already presented in section 3. In contrast, IREC, SAU, and NESSTEC conducted overnight tests at ambient temperature on different sets

Funded by the European Union
Views and opinions expressed are those of the author(s) only and do not necessarily reflect those of the European Union or CINEA. Neither the European Union nor the granting authority can be held responsible for them. This project has received funding from Horizon Europe research and innovation programme under Grant Agreement No.1069890

of cells, focusing on specific evaluations such as SoH and standard testing protocols. The results of IREC will be presented in future deliverable. This collaborative effort ensures a comprehensive assessment of cell performance to support decisions on secondary use and recycling.

4.1. Electrochemical Tests of Lithium Ion Cells dismantled from LMT Modules

Two project partners, NESSTEC and SAKARYA, jointly conducted the electrochemical tests. Eight battery packs were received, disassembled, and evaluated under ambient conditions. Digital images of the disassembled cells are presented in Figure 4.1, where "P" denotes the pack and "C" represents the cell. In total, eight packs comprising 216 cells were examined.

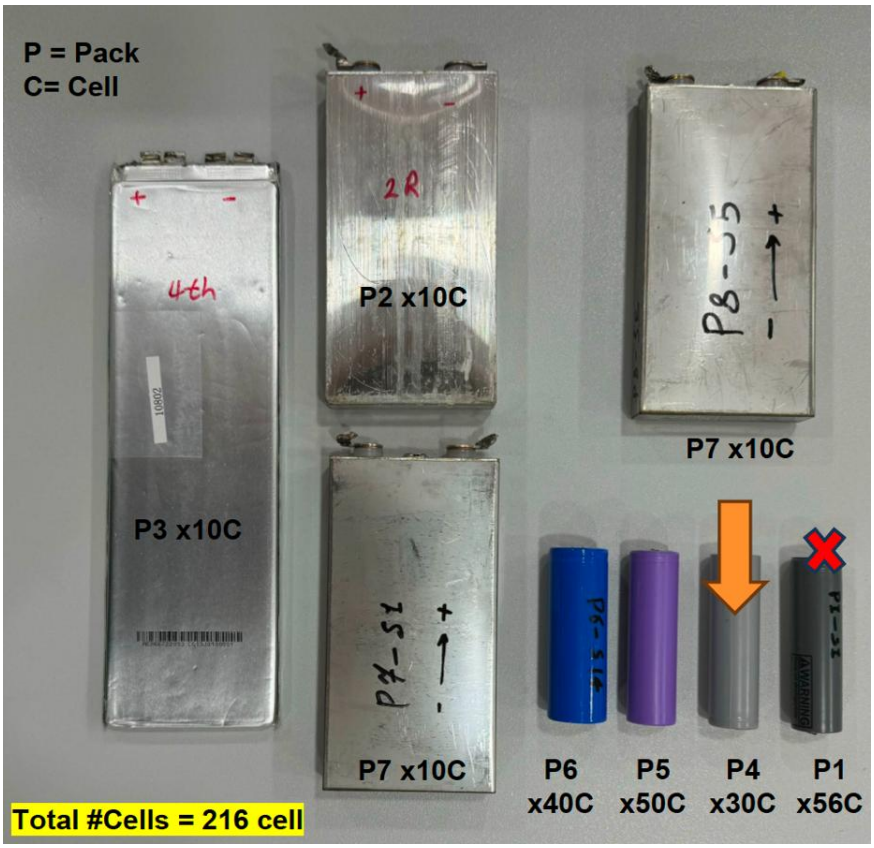

Figure 4.1. *Digital image of dismantled cell samples received by NESSTEC & SAKARYA*

Preliminary tests revealed that Pack 1 was over-discharged (pack voltage = 0 V); specifically, this pack contained 56 cells, each registering 0 V. Additionally, Packs 2, 7, and 8, which consist of prismatic cells, and pack 3 consist of pouch cells, exhibited noticeable swelling, raising significant safety concerns.

Funded by the European Union
Views and opinions expressed are those of the author(s) only and do not necessarily reflect those of the European Union or CINEA. Neither the European Union nor the granting authority can be held responsible for them. This project has received funding from Horizon Europe research and innovation programme under Grant Agreement No.1069890

A subset of cells from Pack 4 underwent further evaluation, including preconditioning, energy and capacity assessments, and open-circuit voltage (OCV) versus state of charge (SOC) tests, in accordance with the established testing protocols. The report highlights the best and worst cell performance results based on measured capacity from Pack 4. Table 4.2 summarize the detailed pack information.

Table 4.2. *Received packs and initial test results*

Pack number	Cell type	Voltage on pack label	Pack voltage V	Cell Voltage	Note
#1	Cylindrical	24V 20A	0 V	0 V	Pack is over discharged
#2	Prismatic	No label	40.2 V	4.2 V	No comment
#3	Pouch	36V 10Ah 360wh	33 V	3.3 V	No comment
#4	Cylindrical	36V 6Ah 216 wh	Not tested	3.57 V	No comment
#5	Cylindrical	No label	37.9 V	3.6 -3.8 V	Some cells were damaged during disassembly
#6	Cylindrical	No label	39.5 V	3.95 V	No comment
#7	Prismatic	No label	7.06 V	3.36 –3.7 V	8 cells not working,2 cells working
#8	Prismatic	No label	34.8 V	3.48 V	No comment

Funded by the European Union

Views and opinions expressed are those of the author(s) only and do not necessarily reflect those of the European Union or CINEA. Neither the European Union nor the granting authority can be held responsible for them. This project has received funding from Horizon Europe research and innovation programme under Grant Agreement No.1069890

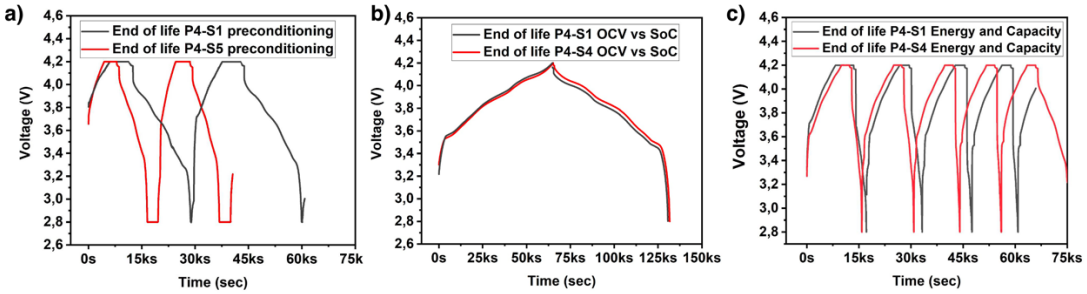

Figure 4.2. a) *Preconditioning,* ***b)*** *OCV vs SoC,* ***c)*** *Energy and Capacity test results of EOL S1 and S5 cells*

Figure 4.2a presents the preconditioning test results for cells S1 and S5, indicating that cell S1 has an approximate capacity of 1.8 Ah, whereas cell S5 exhibits a capacity of only 0.9 Ah. In accordance with the testing protocol, the OCV versus SoC data are depicted in Figure 4.2b, and the corresponding energy and capacity measurements are illustrated in Figure 4.2c.

5. Electrochemical Characterization of Cathode Materials in Coin Cell Level

This section details the electrochemical evaluation of recycled cathode materials integrated into newly assembled lithium-ion cells. The objective is to determine the performance characteristics and viability of recycled electrodes for reuse in battery manufacturing. Both coin and pouch cells fabricated with these materials were subjected to comprehensive electrochemical testing, including charge-discharge cycling, capacity retention, and other key performance metrics. The results not only offer insights into the quality and functionality of the recycled cathode materials but also facilitate direct comparisons with cells produced using commercial-grade electrodes. This analysis is critical for optimizing the recycling processes and advancing the project's broader aim of establishing a sustainable, circular economy in lithium-ion battery production.

Funded by the European Union

Views and opinions expressed are those of the author(s) only and do not necessarily reflect those of the European Union or CINEA. Neither the European Union nor the granting authority can be held responsible for them. This project has received funding from Horizon Europe research and innovation programme under Grant Agreement No.1069890

5.1. Electrochemical Tests of NMC Cathode Material Synthesized via Solid State Method (CP006)

The cathode powder, synthesized by Torrecid via solid state synthesis, was first processed by loading 4.58 mg onto each 12 mm diameter disc. The prepared cathode discs were then dried in a vacuum oven at 110 °C for 24 hours. Subsequently, the discs were incorporated into 2032-coin cells using an electrolyte solution consisting of 1M $LiPF_6$ in a 1:1 (by volume) mixture of EC and DEC (40 µL per coin cell) and a single-layer Celgard 2400 separator. The electrochemical properties of the recycled cathode materials were analyzed using impedance spectroscopy, cyclic voltammetry (CV), and galvanostatic charge-discharge cycling at current rates of C/10 (0.073 mA) and C/2 (0.366 mA) within a potential window of 4.3 to 3.0 V.

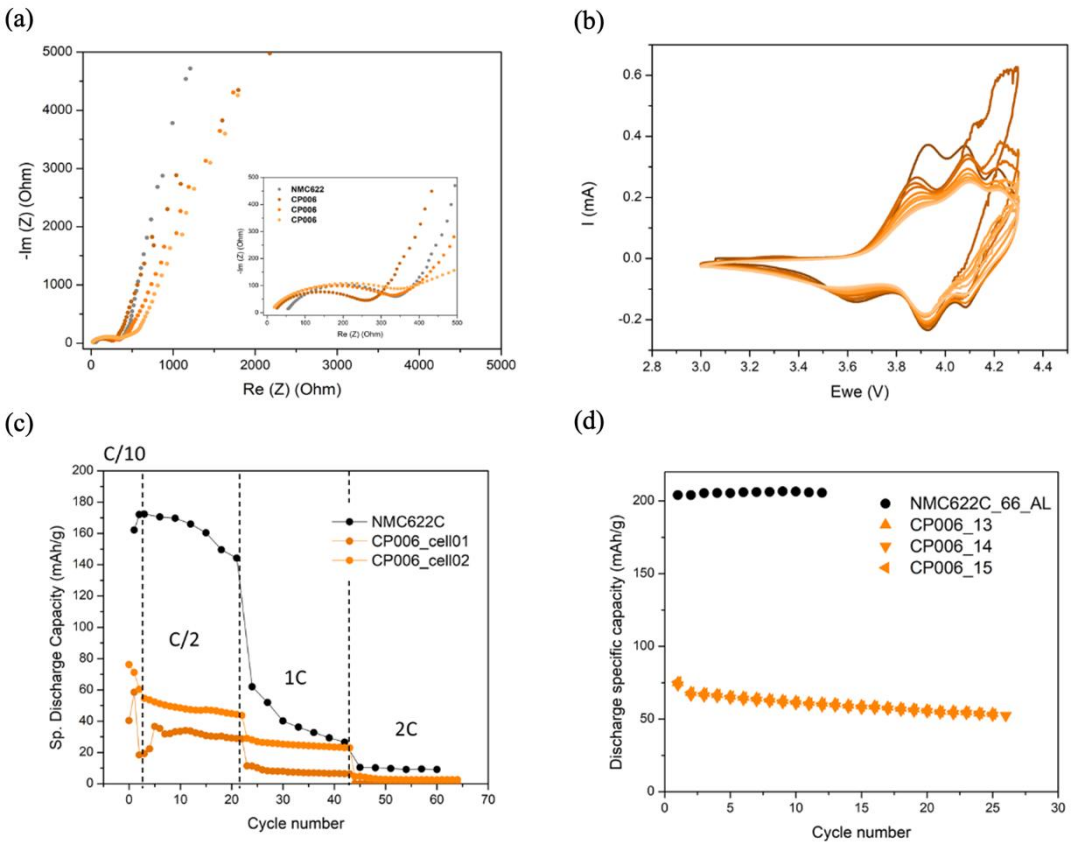

Figure 5.1. a) *Impedance spectroscopy of 3-coin cells of CP006 (orange trace) with respect to commercial NMC622 cathode (grey trace);* ***b)*** *cyclic voltammetry of CP006 cathode;* ***c)*** *comparison of C-rate kinetics with commercial NMC622;* ***d)*** *Discharge specific capacity of 3-half cells with CP006 cathode (orange trace) at C/10 and commercial NMC622 (black trace)*

Funded by the European Union

Views and opinions expressed are those of the author(s) only and do not necessarily reflect those of the European Union or CINEA. Neither the European Union nor the granting authority can be held responsible for them. This project has received funding from Horizon Europe research and innovation programme under Grant Agreement No.1069890

6-coin cells are prepared with the conditions mentioned above. All cells have low resistance (200-300 ohms). Half-cells with recycled cathode material are exposed to 2 formation cycles at C/20, and cycling is performed at C/10 (Figure 5.1d). Compared to commercial NMC622 cathode material, CP006 gives almost half of the capacity (~75mAh/g at C/10). On the C-rate kinetics, CP006 shows a stable but low-capacity trend as well at C/2, 1C, and 2C rates.

5.2. Electrochemical test of LMNO Cathode Material (CP012, CP014, CP031, CP035, CP037)

The tested materials were obtained from recycled precursors (CP012, CP014, CP037), commercial precursors (CP031), and compared with a commercial material (CP035). All of these were provided or synthesized by TORREDCID.

For electrode preparation, the active material (LMNO-CP0), conductive additive (Super P), and binder (PVDF) were mixed in a weight ratio of 90:5:5. The slurry was then coated onto an aluminum current collector and dried in a vacuum oven at 110°C for 24 hours. The electrode was then cut into discs with a diameter of 12 mm.

Subsequently, 2032 Al-coin cells were assembled using the dried cathode discs, with a single-layer Celgard 2400 separator and 36 µL of an electrolyte solution consisting of 1 M $LiPF_6$ in a 1:1 (by volume) mixture of EC and DEC. Electrochemical analyses were conducted using a BioLogic multichannel potentiostat/galvanostat. The characterization techniques included cyclic voltammetry (CV) at a scan rate of 50 $\mu V \cdot s^{-1}$ over a potential range of 3 V to 4.9 V, potentio electrochemical impedance spectroscopy (PEIS) over a frequency range of 0.01 Hz to 10 kHz, and galvanostatic charge-discharge cycling of Li/LMNO cells at various C-rates, with cell cut-off voltages set at 4.9 V for charging and 3.5 V for discharging.

Cyclic Voltammetry (CV) results are shown in Figure 5.2. The typical CV profile for the cubic LNMO is shown in Figure 5.2 a). The main anodic/cathodic contributions are highlighted in the CV curves, as discussed in **Y. Xue et al.**[1] There are two anodic peaks around 4.7 - 4.9 V, which are attributed to a $Ni^{2+/}Ni^{4+}$ redox couple, and the weak peaks at 4.0 V are attributed to a $Mn^{3+/}Mn^{4+}$ redox couple. The peaks are reversible during reduction. These

[1] Y. Xue, Investigation on preparation and performance of spinel $LiNi_{0.5}Mn_{1.5}O_4$ with different microstructures for lithium-ion batteries, Scientific Reports 5:13299, DOI:10.1038/srep13299

Funded by the European Union

Views and opinions expressed are those of the author(s) only and do not necessarily reflect those of the European Union or CINEA. Neither the European Union nor the granting authority can be held responsible for them. This project has received funding from Horizon Europe research and innovation programme under Grant Agreement No.1069890

redox events are clearly identified in the commercial sample CP035, Figure 5.2 b).

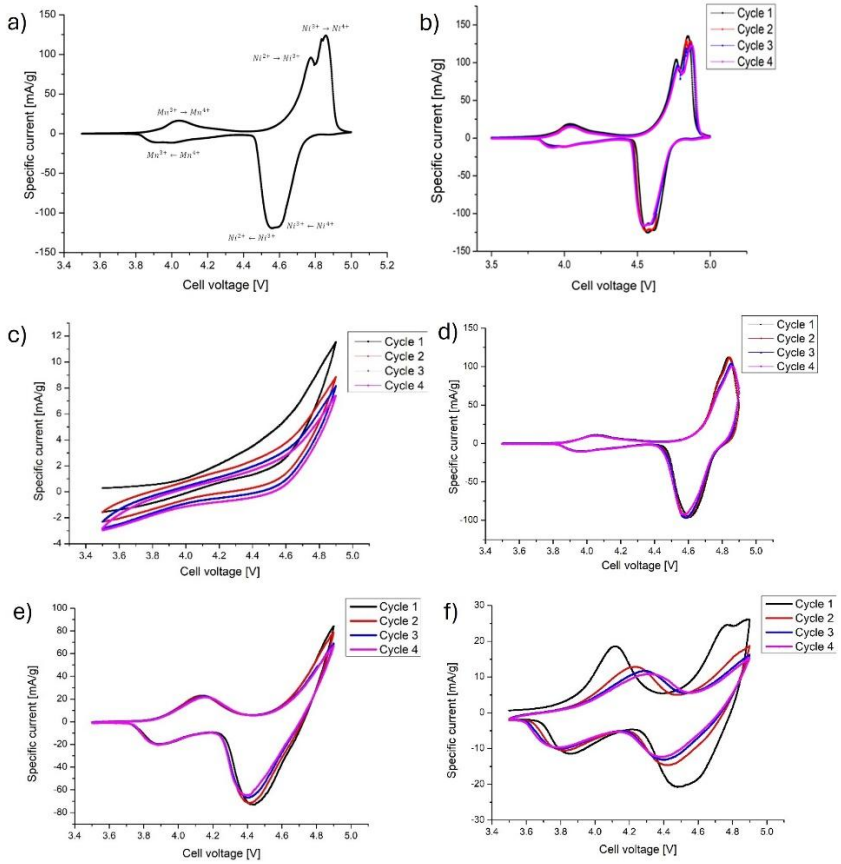

Figure 5.2 *Cyclic Voltammetry of LNMO half-cells at room temperature measured at 50µVs^{-1}:* ***a)*** *as published[1],* ***b)*** *CP035,* ***c)*** *CP012,* ***d)*** *CP014,* ***e)*** *CP031,* ***f)*** *CP037*

For sample CP012, Figure 5.2 c), there are no visible peaks related to the oxidation or reduction of Mn and Ni. This typical profile is generally observed in highly resistive materials with no electrochemical activity. Sample CP014, Figure 5.2 d), displays a similar profile to the reference sample, as it presents the same range of specific current and exhibits the oxidation and reduction peaks of Mn and Ni. The oxidation peaks of Ni are in the range of 4.7 V to 4.8 V, and Mn's peak is at 4.0 V. Finally, the reduction peaks of Ni and Mn are in the ranges of 4.5 V and 3.9 V, respectively. Regarding sample CP031, Figure 5.2 e), the peaks associated with the oxidation of Ni are not clearly defined, but those associated with its reduction are clearly present. In contrast, the oxidation and reduction peaks of Mn are clearly visible and are within the

Funded by the European Union

Views and opinions expressed are those of the author(s) only and do not necessarily reflect those of the European Union or CINEA. Neither the European Union nor the granting authority can be held responsible for them. This project has received funding from Horizon Europe research and innovation programme under Grant Agreement No.1069890

expected ranges for this redox reaction to occur. Sample CP037,5.2 f), shows poor reproducibility between cycles; as cycling progresses, these peaks decrease in intensity and shift to higher potential. Overall, if the peak intensity (mAg^{-1}) for the Ni^{2+}/Ni^{4+} redox activity is considered, the following trend can be observed, from low to high current response: CP012 > CP037 > CP031 > CP014 > CP035 (commercial). From these results, we selected the three best-performing samples, and new coin cells were assembled for galvanostatic charge/discharge and electrochemical impedance spectroscopy studies. The following protocol was applied: 1) measurement of the cell's impedance at its equilibrium potential, 2) two formation cycles at C/10 to activate the cells, 3) cell charging up to 4 V at C/10 and relaxed for impedance measurement, 4) 1 charge/discharge cycle at C/2, 5) cell charging up to 4 V at C/10 and relaxed for impedance measurement, and then repetition from 3) at different C-rates. Results are presented in Figure 5.3.

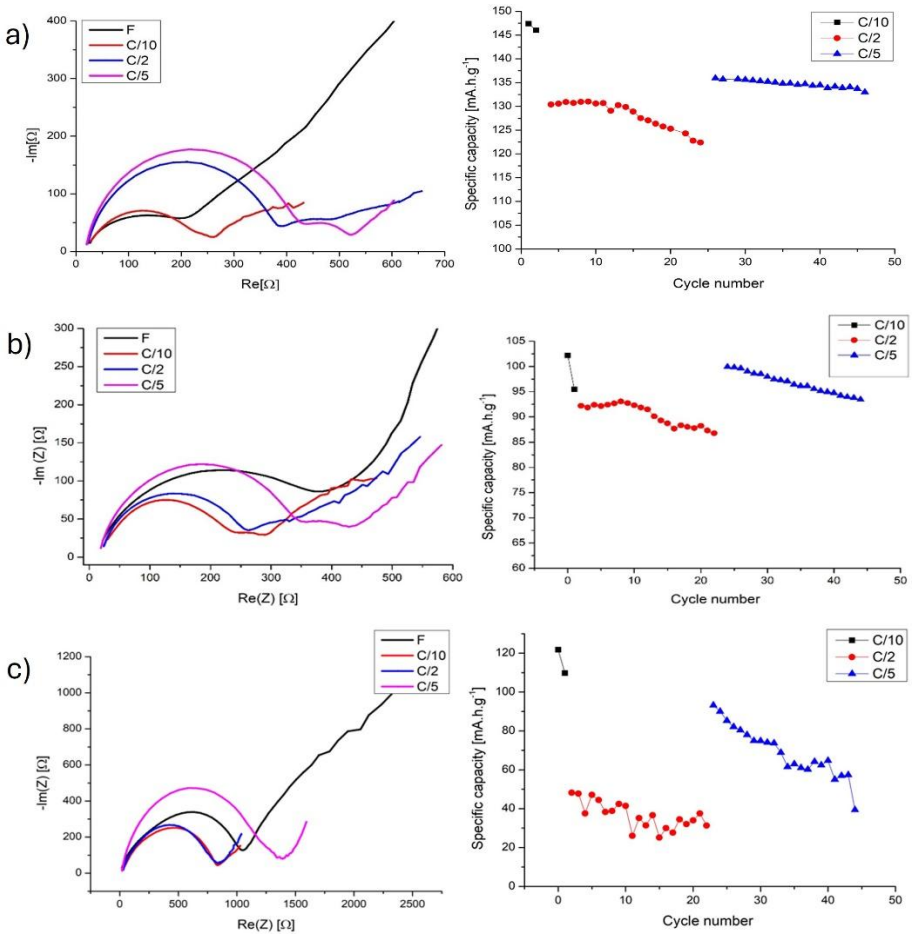

Figure 5.3 *Electrochemical impedance spectroscopy and galvanostatic charge/discharge measurements following protocol defined above of LNMO half-cells at room temperature:* ***a)*** *CP035,* ***b)*** *CP014,* ***c)*** *CP031*

Funded by the European Union

Views and opinions expressed are those of the author(s) only and do not necessarily reflect those of the European Union or CINEA. Neither the European Union nor the granting authority can be held responsible for them. This project has received funding from Horizon Europe research and innovation programme under Grant Agreement No.1069890

The commercial sample CP035 delivers a specific discharge capacity of 147 $mAhg^{-1}$ during activation (2 cycles at C/10), and 134 and 128 $mAhg^{-1}$ at C/5 and C/2, respectively. The associated impedances measured at 4 V as a function of C-rate are 229, 374, and 412 Ω, respectively. Sample CP014 delivers a specific capacity of 98 $mAhg^{-1}$ at C/10 during activation and 96 and 90 $mAhg^{-1}$ at C/5 and C/2, respectively. The associated impedances measured at 4 V as a function of C-rate are 233, 252, and 343 Ω, respectively. Sample CP031 delivers a specific capacity of 115 $mAhg^{-1}$ at C/10, and 70 and 30 $mAhg^{-1}$ at C/5 and C/2, respectively. The associated impedances measured at 4 V as a function of C-rate are 884, 817, and 1260 Ω. The resistance values considered in this study were extracted from the low-frequency Z' intercept of the charge-transfer semicircle.

Regarding LNMO cycling performance, new coin cells were assembled, activated at C/10 for 2 cycles, and then galvanostatically cycled at C/10. The samples analyzed were CP035, CP014, CP031, and CP037. Results are presented in Figure 5.4. Samples CP031 and CP014 show the best performance in capacity retention: 90 % after 100 cycles for CP031 and 90 % for CP014 after 55 cycles. Sample CP037 only delivers 30 % of its initial capacity after 30 cycles.

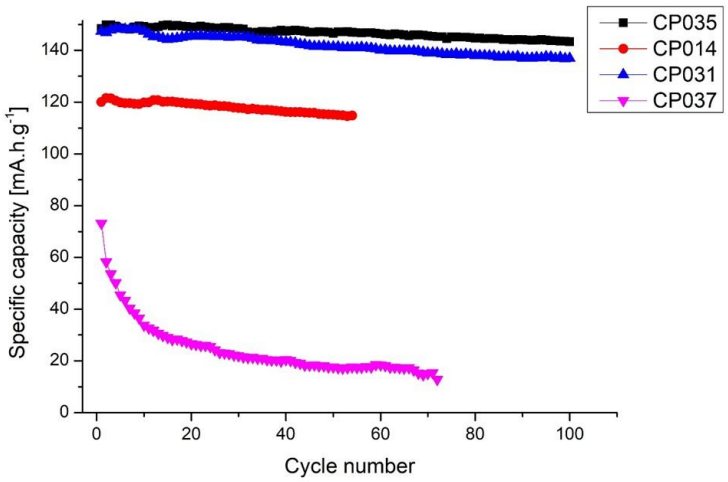

Figure 5.4 *Specific discharge capacity vs. cycle number at C/10 for the samples CP035 (black trace), CP014 (red trace), CP031 (blue trace), and CP037 (pink trace)*

Funded by the European Union

Views and opinions expressed are those of the author(s) only and do not necessarily reflect those of the European Union or CINEA. Neither the European Union nor the granting authority can be held responsible for them. This project has received funding from Horizon Europe research and innovation programme under Grant Agreement No.1069890

5.3. Electrochemical Tests of NMC622 Cathode Material Synthesized by CARTIF via Hydrothermal Synthesis Method (M1, M2, M3)

The material under investigation is an NMC622 cathode powder synthesized by CARTIF via hydrothermal synthesis. Its electrochemical properties were evaluated using impedance spectroscopy, cyclic voltammetry (CV), and galvanostatic charge-discharge cycling at various current densities. For electrode fabrication, three sample sets—M1, M2, and M3—were prepared with cathode loadings of 3.60 mg/disc, 3.86 mg/disc, and 3.08 mg/disc, respectively, using 12 mm diameter discs. The prepared cathode discs were dried in a vacuum oven at 110 °C for 24 hours.

Subsequently, 2032-coin cells were assembled with the dried electrodes, employing a single-layer Celgard 2400 separator and an electrolyte composed of 1 M $LiPF_6$ in a 1:1 (by volume) mixture of EC and DEC (40 µL per coin cell). Galvanostatic charge-discharge tests were conducted at a C/10 current rate, corresponding to 0.0576 mA for M1, 0.0618 mA for M2, and 0.04928 mA for M3, within a potential window of 4.3 V to 3.0 V.

Funded by the European Union

Views and opinions expressed are those of the author(s) only and do not necessarily reflect those of the European Union or CINEA. Neither the European Union nor the granting authority can be held responsible for them. This project has received funding from Horizon Europe research and innovation programme under Grant Agreement No.1069890

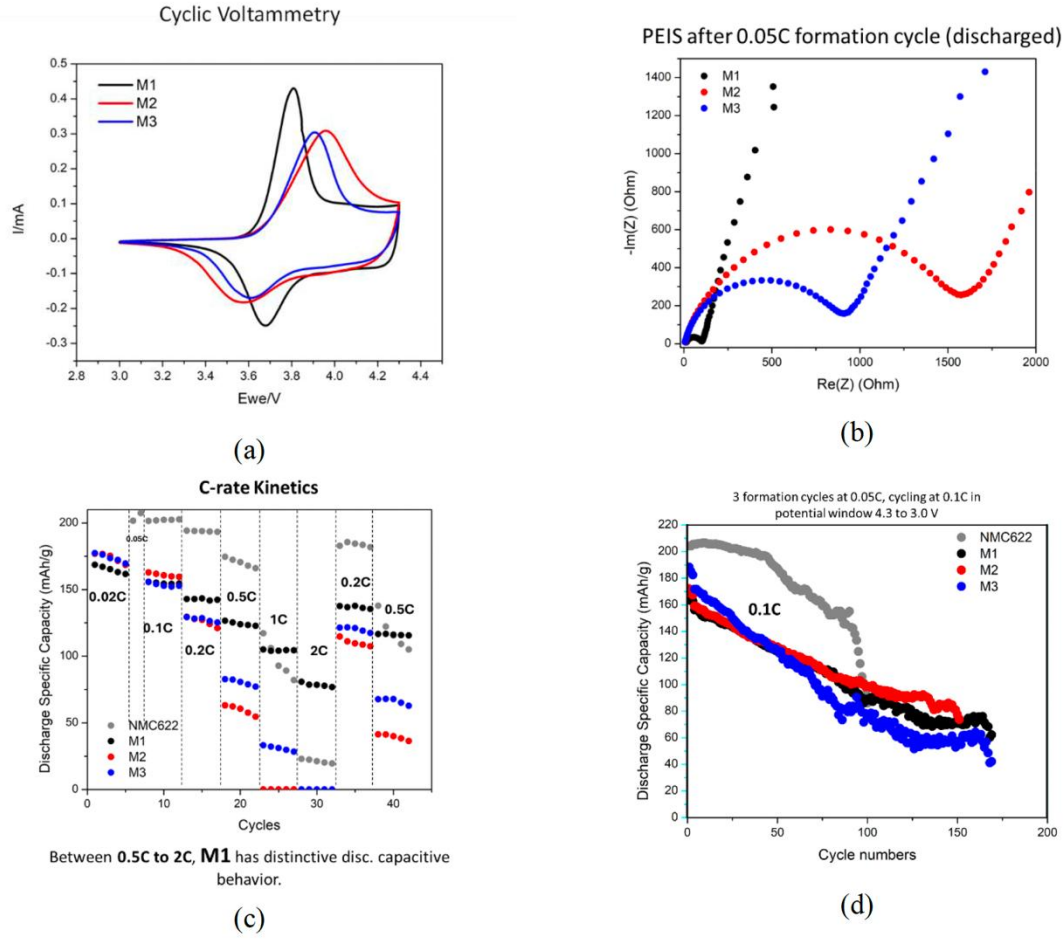

Figure 5.5. a) *Cyclic voltammetry of hydrothermally synthesized cathode materials in half-cell configuration,* ***b)*** *Impedance spectroscopy hydrothermally synthesized samples after formation cycles at 0.05C,* ***c)*** *C-rate kinetics of recycled samples with respect to commercial NMC622,* ***d)*** *long-cycling at 0.1C*

Hydrothermally synthesized NMC622 cathode powders are characterized by cyclic voltammetry between potential 4.3V-3.0V. It is observed that all 3 samples in-line with commercial NMC622 voltammetry. When impedance spectroscopies of these samples are compared it is noticed that M1 has the lowest resistance around 100 Ohms while M2 has the greatest resistance after the formation cycles. To compare C-rate kinetics, every half-cell is measured at different currents and overall behaviour is compared with respect to the commercial NMC622 electrode. Although hydrothermally synthesized samples do not show greater or equal discharge capacity values, it is worth noting that they have quite high and stable discharge specific capacity values. M1 has higher discharge sp. Capacity especially at 0.5C, 1C and 2C among all 3 samples. Furthermore, M1 exhibits the highest discharge specific capacity with 75mAh/g at 2C, which even greater than the commercial NMC622. Also they are exposed to long cycling at 0.1C after following 3 formation cycles at 0.05C.

Funded by the European Union

Views and opinions expressed are those of the author(s) only and do not necessarily reflect those of the European Union or CINEA. Neither the European Union nor the granting authority can be held responsible for them. This project has received funding from Horizon Europe research and innovation programme under Grant Agreement No.1069890

Long cycling at 0.1C shows similar behavior for all 3 samples, showing discharge specific capacity ~150mAh/g in the first 50 cycles. As commercial NMC622 electrode exhibits a sharp decay in the capacity around cycle 100th, hydrothermally synthesized samples M1, M2, M3 maintain stability ~80mAh/g.

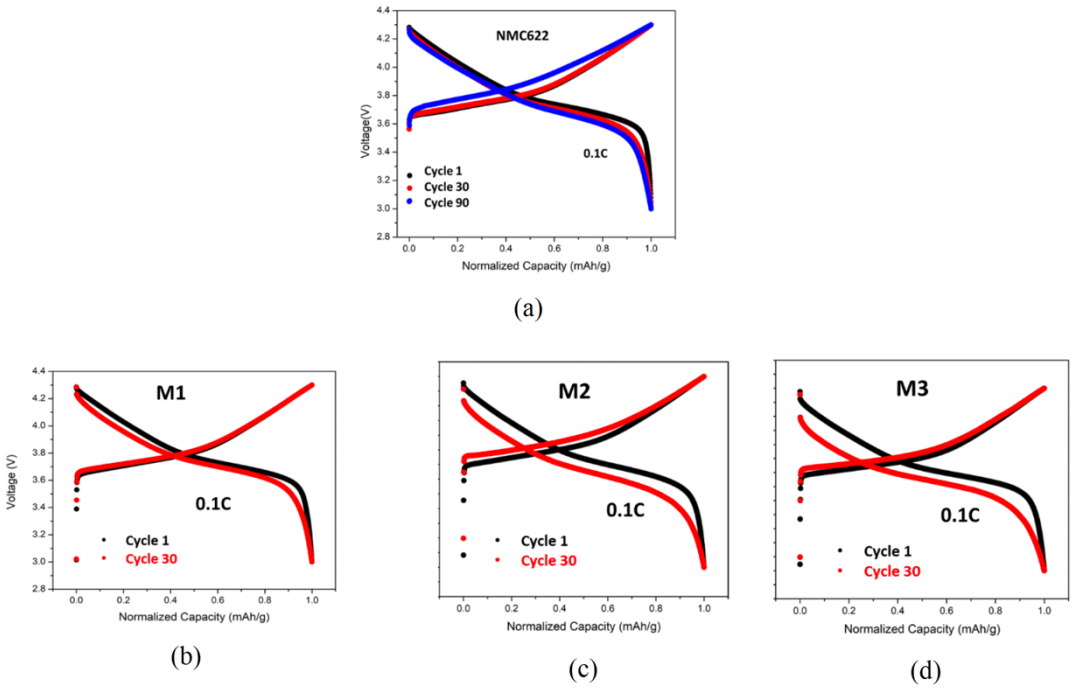

Figure 5.6. *Capacity vs Potential curves of* ***a)*** *commercial NMC622,* ***b)*** *hydrothermally synthesized M1,* ***c)*** *hydrothermally synthesized M2,* ***d)*** *hydrothermally synthesized M3 at 0.1C*

Long cycling results are plotted in capacity vs potential curves, to analyze the cell performance. Although M2 and M3 exhibit lower capacity as the cycling continues, M1 performs very stable and almost identical performance compared to commercial NMC622 at 0.1C, indicating a very promising candidate.

•M1 has the lowest resistance around 100 Ohms while M2 has the greatest resistance
•M1 exhibits the highest discharge specific capacity with 75mAh/g at 2C, which even greater than the commercial NMC622.
•M1 has higher discharge sp. Capacity especially at 0.5C, 1C and 2C among all 3 samples.
•Longer cycling at 0.1C shows similar behavior for all 3 samples, ~150mAh/g in the first 50 cycles.
•Capacity vs potential curve of M1 is almost identical to commercial NMC622 at 0.1C for the 1st and 30th cycles

Funded by the European Union
Views and opinions expressed are those of the author(s) only and do not necessarily reflect those of the European Union or CINEA. Neither the European Union nor the granting authority can be held responsible for them. This project has received funding from Horizon Europe research and innovation programme under Grant Agreement No.1069890

5.4. Electrochemical Tests the Mixture of NMC622 Commercial Cathode and Recycled FRNC34 12 NMC cathode (50:50) (FRNC41)

Torrecid supplied cathode samples produced by blending 50% commercial NMC622 material with recycled components synthesized by CARTIF. NESSTEC conducted the subsequent electrochemical evaluations. Initially, the cathode materials were characterized using X-ray diffraction (XRD) to assess their cation mixing ratios, with the [I(003)/I(104)] ratios ranging from 1.57 to 3.70. The FRNC41 sample, exhibiting a cation mixing ratio closest to the target reference value of 1.2, was selected for rapid preliminary analysis. The electrochemical performance data for both coin cell-type half-cell and full-cell configurations are presented in Figure 5.12.

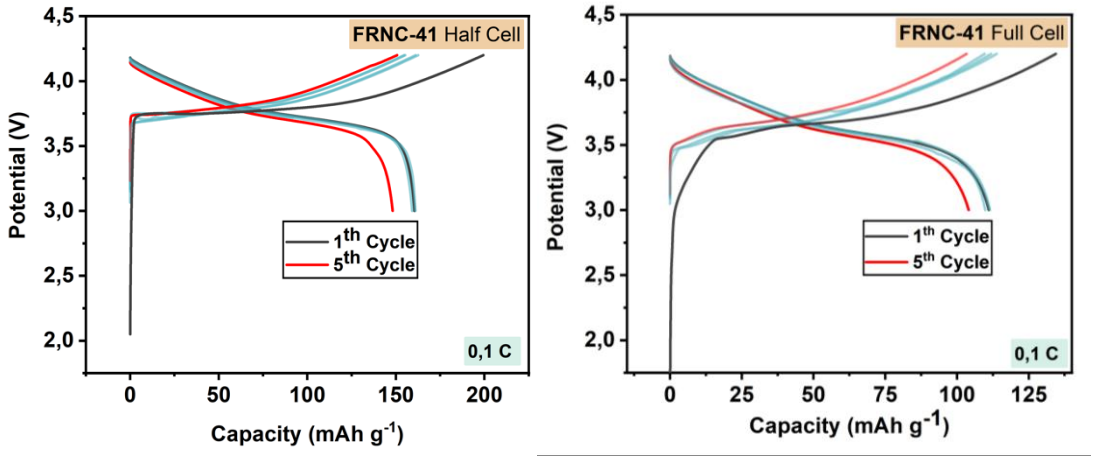

Figure 5.7. *Coin cell type half-cell and full-cell charge-discharge test results*

Two charge–discharge tests were conducted over five cycles at a C-rate of 0.1C within a voltage window of 3.0 V to 4.2 V to evaluate the electrochemical performance of the material under two different cell configurations. In the first configuration, a half-cell was assembled using lithium metal as the counter electrode, while in the second configuration, a full cell was constructed with a commercial graphite anode.

In the half-cell test, the initial discharge capacity was measured at 168 mAh/g. After five cycles, the capacity decreased to 150 mAh/g, indicating a modest capacity fade over the cycling period. In comparison, the full cell exhibited an initial capacity of 113 mAh/g, which declined to 105 mAh/g by the fifth cycle. The lower capacity observed in the full cell is typical due to the intrinsic limitations of the graphite anode and the more complex cell balancing in a full-

Funded by the European Union
Views and opinions expressed are those of the author(s) only and do not necessarily reflect those of the European Union or CINEA. Neither the European Union nor the granting authority can be held responsible for them. This project has received funding from Horizon Europe research and innovation programme under Grant Agreement No.1069890

cell configuration, as opposed to the nearly ideal conditions in a half-cell with a lithium metal counter electrode.

These results suggest that while both configurations show some degree of capacity degradation, the half-cell delivers higher absolute capacity values, likely due to its simpler electrochemical interface. The modest capacity fade across the cycles demonstrates that the material maintains relatively stable performance at the low C-rate of 0.1C. However, further long-term cycling studies would be necessary to fully assess the durability and practical application potential of the electrode material in commercial cell architectures.

5.5. Electrochemical Half-Cell Tests of NMC811, NMC622 cathodes and Graphite Anodes (CP028, CP029, CP030, CP032, CP042, CP043, CP044 cathodes and GRA004 anode)

The recycled cathode powders are coded as CP028, CP029, CP030, CP032, CP042, CP043 (supplied by TORRECID) and CP044 (supplied by LUREDERRA) and are electrochemically tested at the half-cell coin cell level. CP028, CP029, CP030, CP032, CP042, and CP043 cathode powders are in the form of NMC622 and are obtained through the solid-state synthesis method, whereas CP044 cathode powder is in the form of NMC811 and is obtained using the flame pyrolysis synthesis method. The GRA004 anode powders are supplied by CSIC and obtained via BM from FRAUNHOFER after a combined pyro-hydrometallurgical treatment (thermal treatment + water leaching + HCl leaching).

The half-cell coin cell results of CP028, CP029, CP030, and CP032 cathode powders, along with GRA004 anode powders (designated as BM03-2), were previously reported in D3.6. However, the electrochemical charge/discharge results are also included in this deliverable to highlight the differences between half-cell and full-cell results. The electrode preparation parameters (binder type and amount, carbon black and active material content), coin cell assembly conditions (coin cell type, electrolyte volume, separator type), and electrochemical test conditions (galvanostatic charge/discharge tests, cyclic voltammetry, and impedance) are provided in Table (5.1).

Funded by the European Union

Views and opinions expressed are those of the author(s) only and do not necessarily reflect those of the European Union or CINEA. Neither the European Union nor the granting authority can be held responsible for them. This project has received funding from Horizon Europe research and innovation programme under Grant Agreement No.1069890

Table 5.1. *Electrode preparation, coin cell assembling and electrochemical test conditions for anode and cathode powders synthesized samples for FREE4LiB project.*

Half Cell Coin Cell Parameters for Cathode and Anode Powders			
		Cathode powder	**Anode powders**
Electrode preparation	Binder type and amount	PVDF – 10 wt%	CMC – 5 wt%
	Carbon black amount	Super P – 10 wt%	Super P – 5 wt%
	Active material amount	80 wt.%	90 wt.%
	Electrode thickness	Wet thickness ~300 µm	Wet thickness ~300 µm
	Loading (mg/cm2)	~5 mg/cm2	~5 mg/cm2
Coin cell assembly	Coin cell type	2016	2016
	Electrolyte type and volume	60 µl of 1M LiPF6 in EC:DMC	60 µl of 1M LiPF6 in EC:DMC
	Half-cell or full-cell	Half-cell	Half-cell
	Separator	Celgard 2400	Celgard 2400
Electrochemical tests	Charge/discharge test parameters	Voltage range: 4.2-2.7 V vs. Li/Li+ Current: C/20 and C/10	Voltage range: 1.5-0.1 V vs. Li/Li+ Current: C/20 and C/10

Funded by the European Union

Views and opinions expressed are those of the author(s) only and do not necessarily reflect those of the European Union or CINEA. Neither the European Union nor the granting authority can be held responsible for them. This project has received funding from Horizon Europe research and innovation programme under Grant Agreement No.1069890

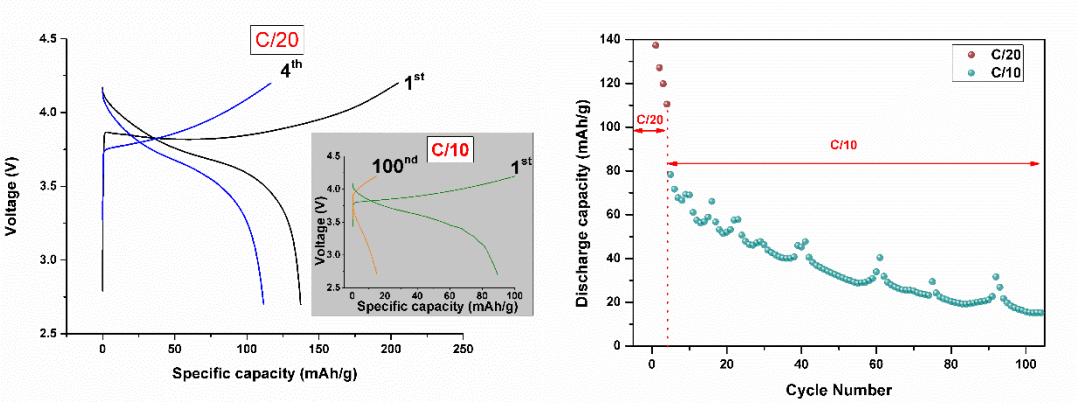

Figure 5.8. *Electrochemical galvanostatic charge/discharge curves and cycle performances of CP028 sample.*

Figure (5.8) presents the electrochemical galvanostatic charge/discharge results for the CP028 sample using a half-cell coin cell configuration. At a C/20 rate, the initial cycle exhibited a discharge capacity of 137 mAh g^{-1}, which decreased to 100 mAh g^{-1} by the fourth cycle. However, long-term cycling tests conducted at a C/10 rate revealed a significant decline in capacity, reaching 15 mAh g^{-1} by the 104th cycle.

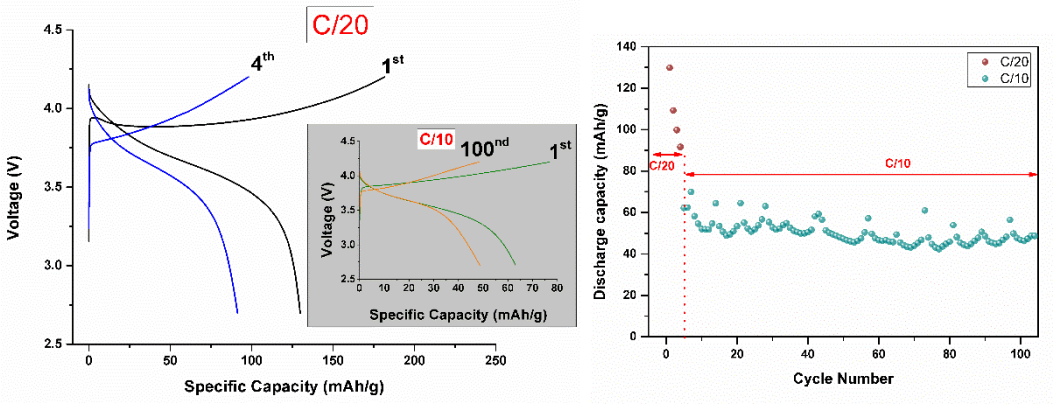

Figure 5.9. *Electrochemical galvanostatic charge/discharge curves and cycle performances of CP029 sample.*

Figure (5.9) illustrates the electrochemical galvanostatic charge/discharge results for the CP029 sample. At a C/20 rate, the first cycle showed a discharge capacity of 129 mAh g^{-1}, which dropped to 91 mAh g^{-1} by the fourth cycle. Continued cycling at a C/10 rate resulted in a gradual capacity fade, with the value decreasing to 48 mAh g^{-1} by the 104th cycle.

Funded by the European Union

Views and opinions expressed are those of the author(s) only and do not necessarily reflect those of the European Union or CINEA. Neither the European Union nor the granting authority can be held responsible for them. This project has received funding from Horizon Europe research and innovation programme under Grant Agreement No.1069890

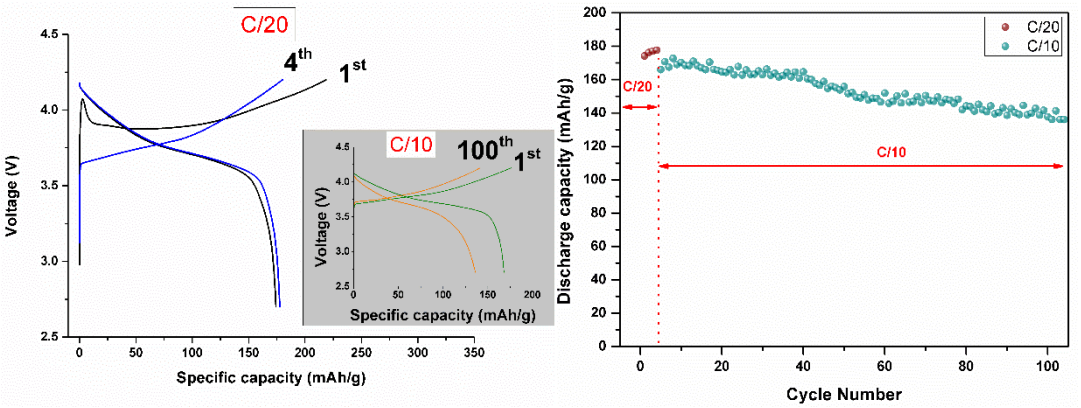

Figure 5.10. *Electrochemical galvanostatic charge/discharge curves and cycle performances of CP030 sample.*

As shown in Figure (5.10), the CP030 sample demonstrated an initial discharge capacity of 174 mAh g^{-1} at a C/20 rate, which slightly increased to 177 mAh g^{-1} by the fourth cycle. Unlike the previous samples, CP030 exhibited improved stability, maintaining a capacity of 136 mAh g^{-1} after 104 cycles at a C/10 rate.

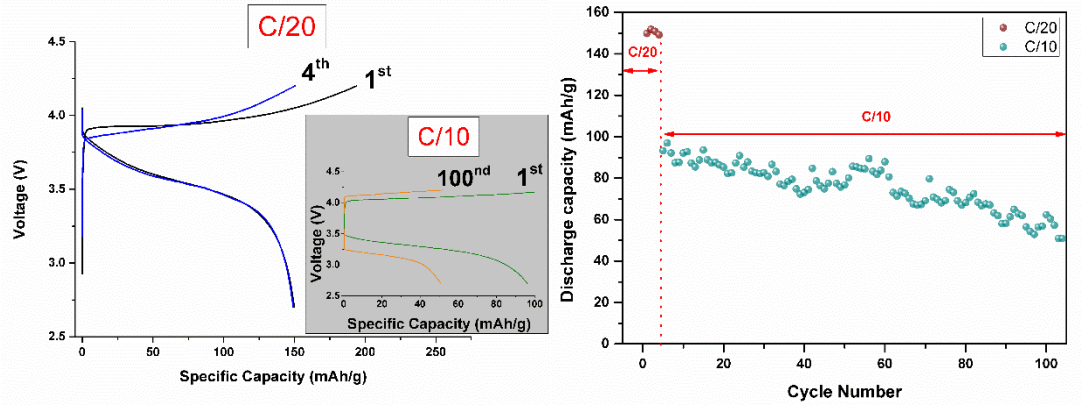

Figure 5.11. *Electrochemical galvanostatic charge/discharge curves and cycle performances of CP032 sample.*

The electrochemical charge/discharge performance of the CP032 sample is presented in Figure (5.11). At a C/20 rate, both the first and fourth cycles exhibited a discharge capacity of 149 mAh g^{-1}. However, capacity degradation was observed in long-term cycling at a C/10 rate, where the value dropped to 50 mAh g^{-1} by the 104th cycle.

Funded by the European Union

Views and opinions expressed are those of the author(s) only and do not necessarily reflect those of the European Union or CINEA. Neither the European Union nor the granting authority can be held responsible for them. This project has received funding from Horizon Europe research and innovation programme under Grant Agreement No.1069890

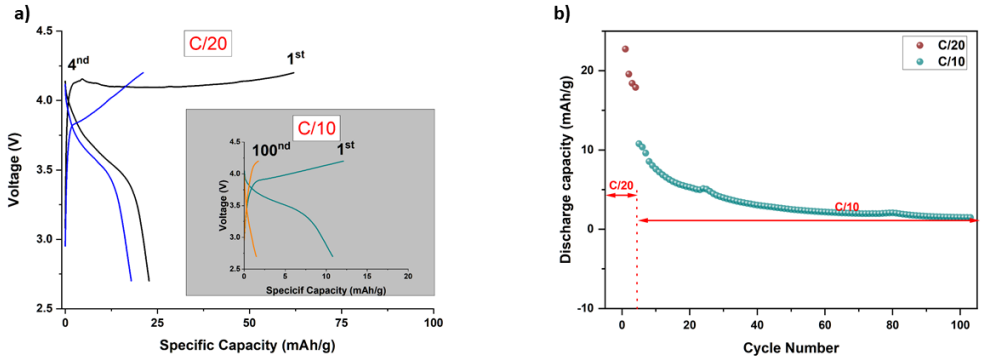

Figure 5.12. *Electrochemical galvanostatic charge/discharge curves and cycle performances of CP042 sample.*

Figure (5.12) depicts the electrochemical performance of the CP042 sample. This sample demonstrated an initial discharge capacity of 14 mAh g^{-1} at a C/20 rate, which drastically declined to 2 mAh g^{-1} by the fourth cycle. Further cycling at a C/10 rate resulted in a negligible capacity of 1 mAh g^{-1} by the 104th cycle, indicating severe capacity fading.

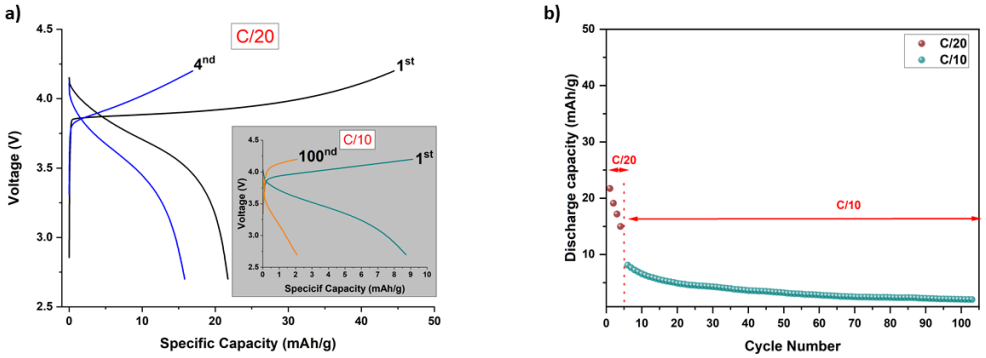

Figure 5.13. *Electrochemical galvanostatic charge/discharge curves and cycle performances of CP043 sample.*

Figure (5.13) displays the electrochemical charge/discharge performance of the CP043 sample. The initial discharge capacity at a C/20 rate was 22 mAh g^{-1}, reducing to 15 mAh g^{-1} by the fourth cycle. Long-term cycling at a C/10 rate resulted in a significant decline, with a final capacity of 2 mAh g^{-1} at the 104th cycle.

Funded by the European Union

Views and opinions expressed are those of the author(s) only and do not necessarily reflect those of the European Union or CINEA. Neither the European Union nor the granting authority can be held responsible for them. This project has received funding from Horizon Europe research and innovation programme under Grant Agreement No.1069890

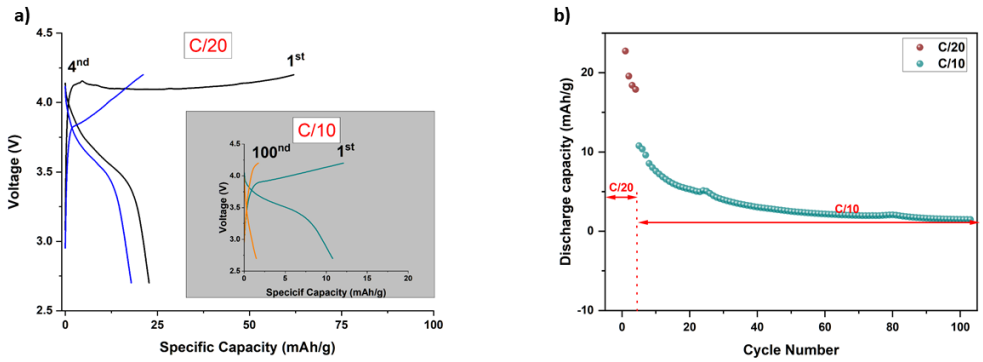

Figure 5.14. *Electrochemical galvanostatic charge/discharge curves and cycle performances of CP044 sample.*

Figure (4.14) presents the electrochemical performance of the CP044 sample. At a C/20 rate, the initial discharge capacity was 22 mAh g^{-1}, which slightly declined to 18 mAh g^{-1} by the fourth cycle. However, during prolonged cycling at a C/10 rate, the discharge capacity significantly diminished, reaching 1.5 mAh g^{-1} by the 104th cycle.

5.6. Electrochemical Full-Cell Tests of NMC811, NMC622 cathodes and Graphite Anodes (CP028, CP029, CP030, CP032, cathodes and GRA004 anode)

Due to the low discharge capacities obtained in the half-cell tests of CP042, CP043, and CP044, full-cell tests were not carried out. Instead, full-cell tests were conducted using CP028, CP029, CP030, and CP032 cathode powders, which exhibited higher potential, along with GRA004 anode powders, based on the data provided in Table 4.2. Table 4.2 details the electrode preparation from anode and cathode powders. For the full-cell tests of recycled cathode materials, commercial graphite was used as the anode, while for the full-cell tests of recycled anode powders, commercial NMC622 cathode material was used. The parameters utilized for charge and discharge tests are also provided in Table 5.2.

Funded by the European Union
Views and opinions expressed are those of the author(s) only and do not necessarily reflect those of the European Union or CINEA. Neither the European Union nor the granting authority can be held responsible for them. This project has received funding from Horizon Europe research and innovation programme under Grant Agreement No.1069890

Table 5.2. *Electrode preparation, coin cell assembling and electrochemical test conditions for anode and cathode powders synthesized samples for FREE4LiB project.*

Full Cell Coin Cell Parameters for Cathode and Anode Powders			
		Cathode powder	**Anode powders**
Electrode preparation	Binder type and amount	PVDF – 5 wt%	CMC – 5 wt%
	Carbon black amount	Super P – 5 wt%	Super P – 5 wt%
	Active material amount	90 wt.%	90 wt.%
	Electrode thickness	Wet thickness ~300 µm	Wet thickness ~150 µm
	Loading (mg/cm2)	~5 mg/cm2	~2.5 mg/cm2
Coin cell assembly	Coin cell type	2016	2016
	Electrolyte type and volume	60 µl of 1M LiPF6 in EC:DMC	60 µl of 1M LiPF6 in EC:DMC
	Half-cell or full-cell	Half-cell	Half-cell
	Separator	Celgard 2400	Celgard 2400
Electrochemical tests	Charge/discharge test parameters	Voltage range: 4.2-2.7 V vs. Li/Li+ Current: C/20 and C/10	

Funded by the European Union

Views and opinions expressed are those of the author(s) only and do not necessarily reflect those of the European Union or CINEA. Neither the European Union nor the granting authority can be held responsible for them. This project has received funding from Horizon Europe research and innovation programme under Grant Agreement No.1069890

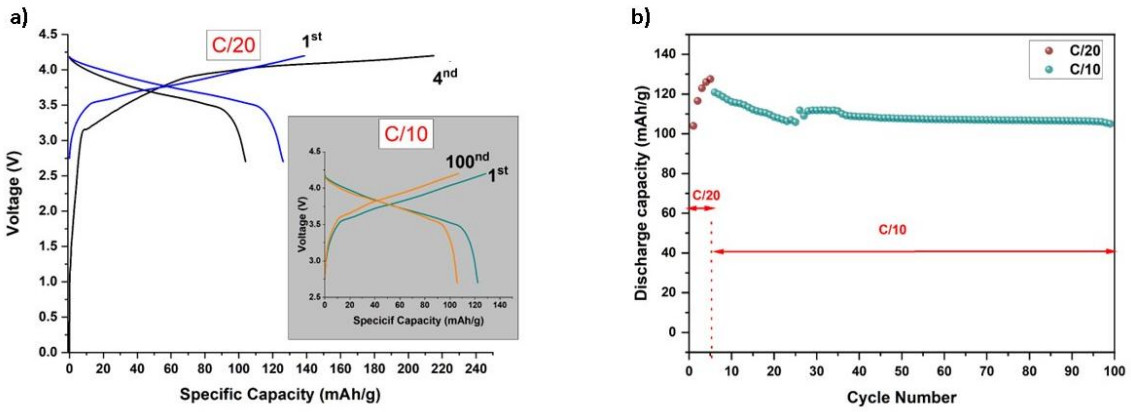

Figure 5.15. *Full-cell electrochemical galvanostatic charge/discharge curves and cycle performances of commercial NMC622 and commercial artificial graphite sample.*

Figure 5.15 presents the galvanostatic charge and discharge results of Li-ion full cells prepared with commercial NMC622 cathode and commercial artificial graphite anode materials. The initial discharge capacity at a C/20 C-rate was measured as 104 mAh g^{-1}, increasing to 127 mAh g^{-1} by the 4th cycle. When the test continued at a C/10 C-rate, the discharge capacity remained stable at 105 mAh g^{-1}.

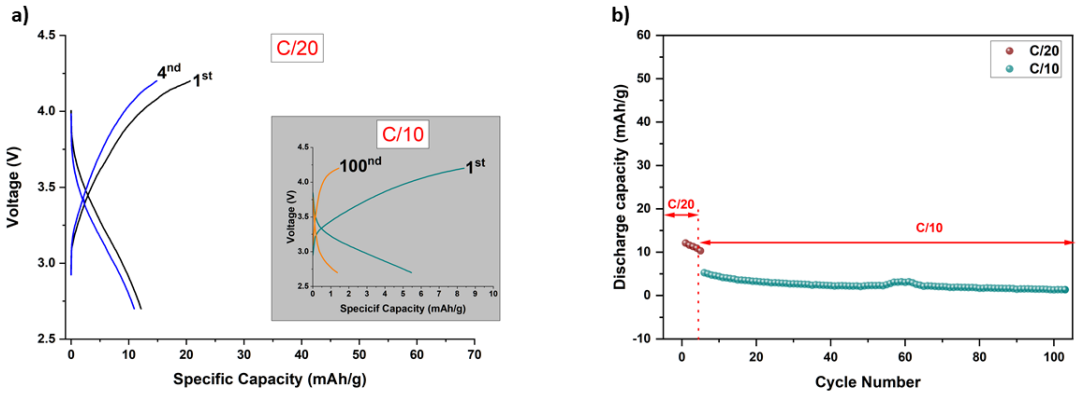

Figure 5.16. *Full-cell electrochemical galvanostatic charge/discharge curves and cycle performances of CP028 sample.*

The full-cell galvanostatic charge/discharge curves for the CP028 sample are shown in Figure 5.16. The test results indicate that the initial discharge capacity at a C/20 C-rate was 12 mAh g^{-1}, while the capacity at the 4th cycle was 10 mAh g^{-1}. At the 104th cycle with a C/10 C-rate, the discharge capacity dropped to approximately 1 mAh g^{-1}.

Funded by the European Union

Views and opinions expressed are those of the author(s) only and do not necessarily reflect those of the European Union or CINEA. Neither the European Union nor the granting authority can be held responsible for them. This project has received funding from Horizon Europe research and innovation programme under Grant Agreement No.1069890

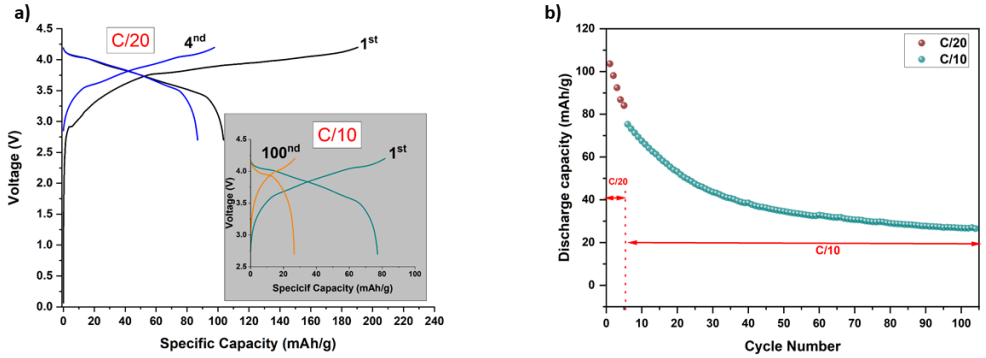

Figure 5.17. *Full-cell electrochemical galvanostatic charge/discharge curves and cycle performances of CP029 sample.*

The full-cell galvanostatic charge/discharge curves for the CP029 sample are presented in Figure 5.17. The initial discharge capacity at a C/20 C-rate was found to be 103 mAh g^{-1}, decreasing to 84 mAh g^{-1} at the 4th cycle. By the 104th cycle at a C/10 C-rate, the discharge capacity declined to 26 mAh g^{-1}.

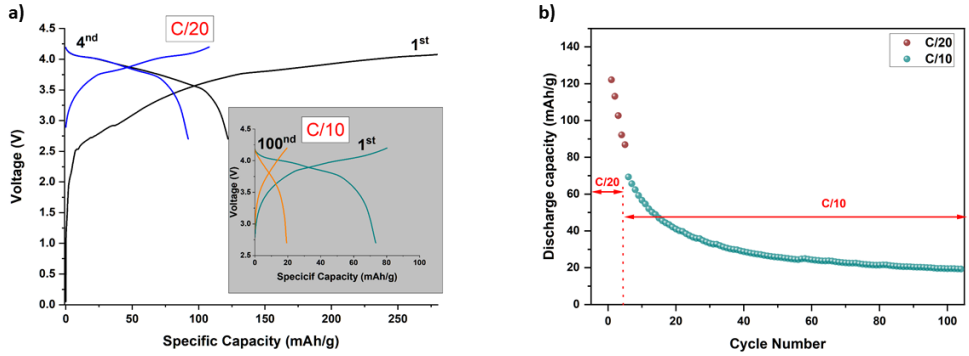

Figure 5.18. *Full-cell electrochemical galvanostatic charge/discharge curves and cycle performances of CP030 sample.*

Figure 5.18 illustrates the full-cell galvanostatic charge/discharge curves for the CP030 sample. The test results reveal that the initial discharge capacity at a C/20 C-rate was 122 mAh g^{-1}, with a decrease to 86 mAh g^{-1} by the 4th cycle. By the 104th cycle at a C/10 C-rate, the discharge capacity dropped to 19 mAh

Funded by the European Union

Views and opinions expressed are those of the author(s) only and do not necessarily reflect those of the European Union or CINEA. Neither the European Union nor the granting authority can be held responsible for them. This project has received funding from Horizon Europe research and innovation programme under Grant Agreement No.1069890

g^{-1}.

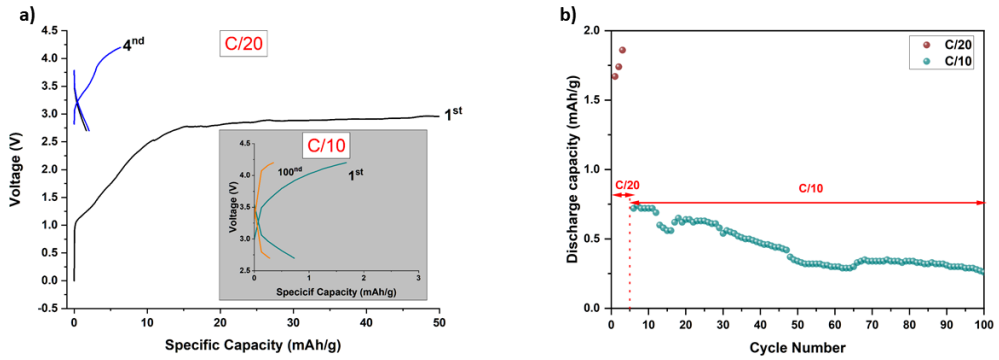

Figure 5.19. *Full-cell electrochemical galvanostatic charge/discharge curves and cycle performances of CP032 sample.*

The full-cell galvanostatic charge/discharge curves for the CP032 sample are shown in Figure 5.19. The initial discharge capacity at a C/20 C-rate was recorded as 1.5 mAh g^{-1}, reaching 2 mAh g^{-1} by the 4th cycle. However, by the 104th cycle at a C/10 C-rate, the discharge capacity diminished to 0.3 mAh g^{-1}.

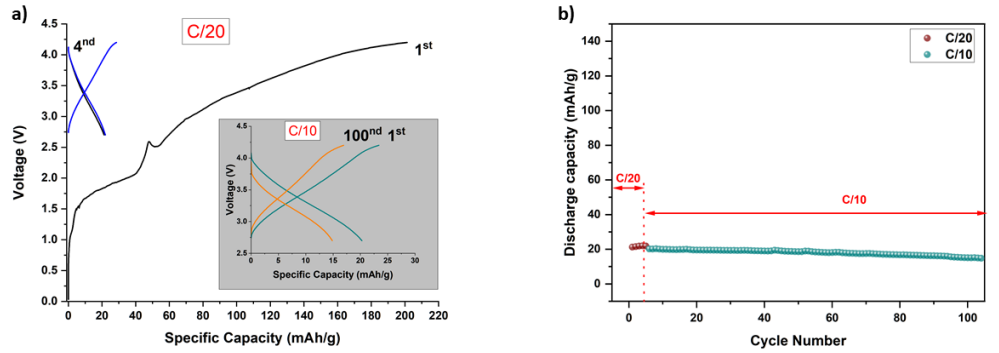

Figure 5.20. *Full-cell electrochemical galvanostatic charge/discharge curves and cycle performances of GRA004 anode sample.*

The full-cell galvanostatic charge/discharge test results for the anode material initially coded as BM03-2 but later renamed GRA004 are presented in Figure 5.20. Despite achieving high capacities in half-cell tests, the expected results were not obtained in full-cell tests. The studies conducted at both C/20 and C/10 C-rates yielded a discharge capacity of approximately 20 mAh g^{-1}. This discrepancy is attributed to the fact that lithium metal was used as the counter electrode in the half-cell tests, whereas commercial NMC622 was employed in the full-cell tests, leading to a lower Li-ion concentration. Additionally, in half-cell tests, the impact of impurities within the powder on battery performance is relatively lower compared to full-cell tests, which could also explain this outcome. Furthermore, since graphite structures remaining from inorganic

Funded by the European Union

Views and opinions expressed are those of the author(s) only and do not necessarily reflect those of the European Union or CINEA. Neither the European Union nor the granting authority can be held responsible for them. This project has received funding from Horizon Europe research and innovation programme under Grant Agreement No.1069890

acid leaching are present, morphology does not exhibit the desired properties, posing another factor that negatively affects full-cell battery performance.

As a conclusion, the performance comparison of full-cell tests reveals that cells prepared with commercial NMC622 cathode and artificial graphite anode exhibited higher and more stable discharge capacities compared to those using recycled materials. The commercial samples maintained a stable capacity of 105 mAh g^{-1} at a C/10 C-rate, whereas the recycled material-based cells demonstrated significant capacity fading over cycling. The rapid degradation in recycled samples suggests challenges related to material purity, Li-ion availability, and structural stability. Further optimization of the recycling process is necessary to enhance electrochemical performance and extend the cycle life of these materials in practical applications.

6. Scale-Up of Lithium-Ion Cells to Pouch Cell Configurations

FREE4LiB targets the transition from laboratory-scale coin cells to commercially relevant pouch cell formats. The scale-up process aims to validate the performance of the electrode materials and cell assembly protocols under conditions that closely replicate practical applications. Pouch cells, designed to accommodate increased capacities and optimized architectures, were assembled and subjected to comprehensive electrochemical testing. These tests evaluate key performance metrics, such as capacity, cycling stability, and safety, thereby providing critical insights for refining battery pack designs in subsequent work packages.

6.1. Pouch Cell optimization of the FRNC41 Cathode

NESSTEC assembled 300 mAh pouch cells employing a stacking method. The process began with electrode preparation, where both anode and cathode electrodes were fabricated using a slurry formulated with a 90:5:5 ratio of active material, Super P conductive additive, and binder, with a 200 µm wet gap maintained during coating to ensure uniform thickness. The coated electrode sheets were then precision-cut into dimensions of 56 x 43 mm, and terminal tabs were fashioned to 11 x 14 mm to facilitate electrical connections.

Funded by the European Union

Views and opinions expressed are those of the author(s) only and do not necessarily reflect those of the European Union or CINEA. Neither the European Union nor the granting authority can be held responsible for them. This project has received funding from Horizon Europe research and innovation programme under Grant Agreement No.1069890

Following cutting, nickel (Ni) and aluminum (Al) tabs were ultrasonically welded to the respective electrodes to secure low-resistance electrical contacts.

The cell components were subsequently assembled in a stacking configuration, with layers arranged in the order of cathode, separator, and anode, ensuring proper alignment of the terminal tabs for optimal contact. The electrode stack was then inserted into an aluminum laminated film, which was heat-sealed along three sides, leaving one side open for electrolyte injection. The open pouch was filled with a 1.5 M $LiPF_6$ solution in an EC:DMC (1:1 by weight) electrolyte, and following this, the pouch was vacuum sealed to achieve an airtight enclosure. Finally, the completed pouch cells were subjected to electrochemical testing to verify their performance and capacity.

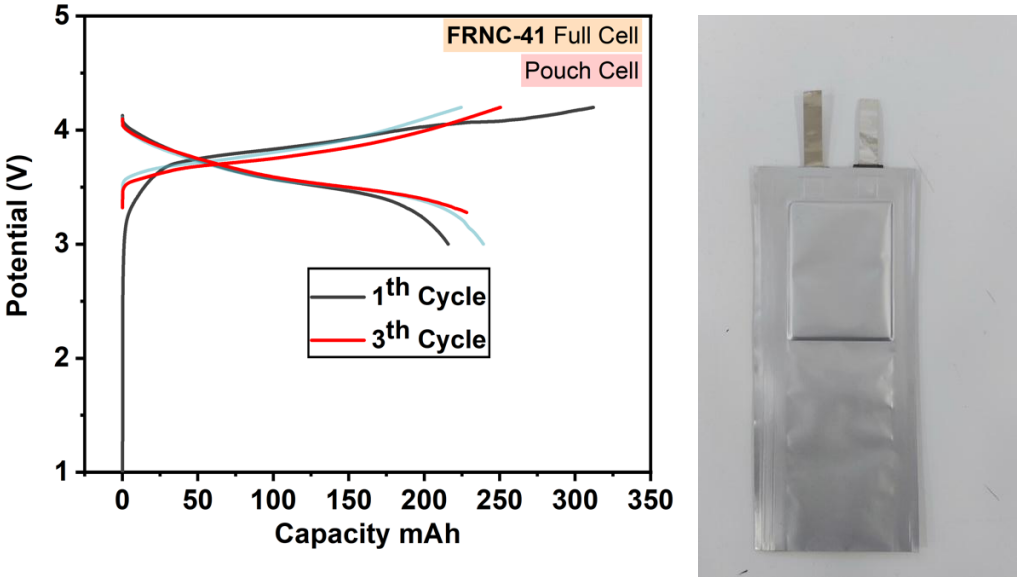

Figure 6.1. *300 mAh pouch cell charge-discharge test results (FRNC41 recycled cathode) with the digital image of the cell*

The electrochemical characterization of the pouch cells, assembled by FRNC41 cathode cycled between 3 V and 4.2 V, revealed an initial charge capacity of 320 mAh and a first discharge capacity of 220 mAh, indicating an initial irreversible capacity loss. Notably, the discharge capacity increased to 250 mAh in the second cycle and continued to rise in the third cycle. This trend suggests that the cell undergoes an activation process during the early cycles, likely due to improved electrode wetting, stabilization of the solid electrolyte interface (SEI), and enhanced utilization of the active material. Overall, the increasing discharge capacity over the initial cycles indicates a stabilization of cell performance, which is promising for the long-term electrochemical behavior of the pouch cells.

Funded by the European Union

Views and opinions expressed are those of the author(s) only and do not necessarily reflect those of the European Union or CINEA. Neither the European Union nor the granting authority can be held responsible for them. This project has received funding from Horizon Europe research and innovation programme under Grant Agreement No.1069890

6.2. Pouch Cell Scale Up Optimization with Commercial Materials

In the scope of the FREE4LiB, reference pouch cells with commercial materials optimized to design the battery pack and used for final stage. Cathode slurries were prepared with the appropriate amount of NMC 622, Carbon black and PVDF content (90:5:5 % wt.). NMP were used as a solvent. Prepared slurry was coated on Al foil by Dr. Blade with the 320 µm gap. Anode slurries were prepared with the appropriate amount of Graphite, Carbon Black and CMC content (90:5:5 % wt.). Distilled water was used as a solvent. Prepared slurry was coated on Cu foil by Dr. Blade with the 200 µm gap. Produced electrodes were cut (118 x 67 mm electrode and 17 x 17 mm terminal tab dimensions) with electrode die cutter. After stacking electrodes with semi-automatic stacking machine by using PP separator, three sides were sealed with Al laminated film and after drying 80°C in Argon filled glove-box, pouch cell was filled with the appropriate amount of commercial electrolyte (1,5M $LiPF_6$ EC:DMC 1:1 %wt). Electrochemical tests were performed with Neware Battery testing device. All produced cells were aged under the 0,05 C charge-discharge step.

3 Ah pouch cells were prepared for optimization and up to 10 Ah pouch cells prepared for final design. 0.1 C charge discharge test results and digital image of the pouch cell are presented in Figure 6.2.

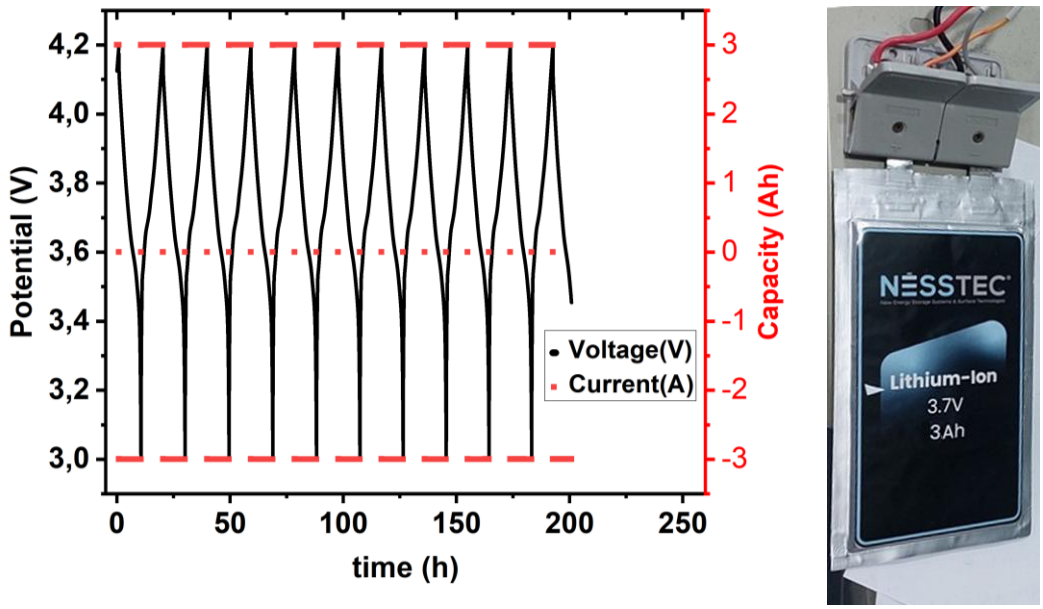

Figure 6.2. *Digital image of the 3Ah pouch cell and its Time-Voltage-Capacity electrochemical test result.*

Funded by the European Union

Views and opinions expressed are those of the author(s) only and do not necessarily reflect those of the European Union or CINEA. Neither the European Union nor the granting authority can be held responsible for them. This project has received funding from Horizon Europe research and innovation programme under Grant Agreement No.1069890

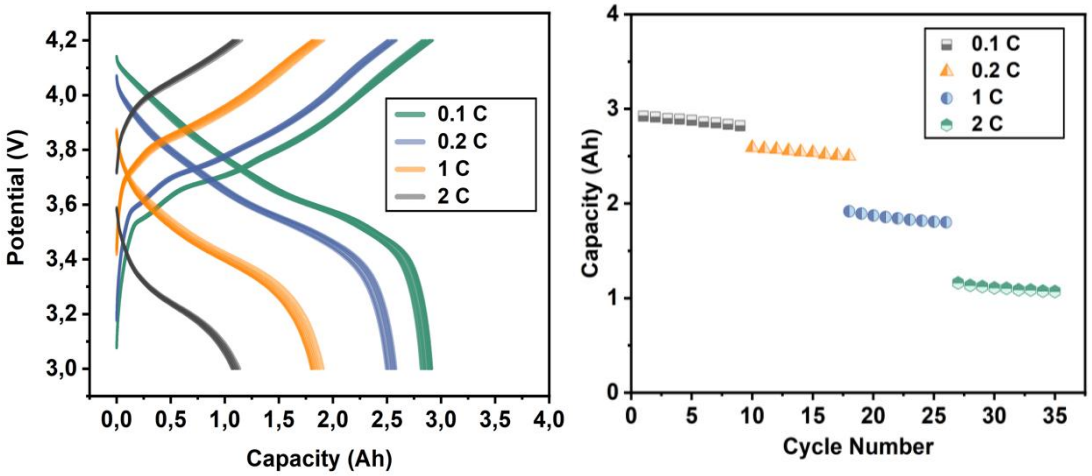

Figure 6.3. *C-Rate performance of 3 Ah pouch cell*

The electrochemical performance tests under different C-rates (0.1C, 0.2C, 1C, and 2C) within a voltage window of 3 V to 4.2 V reveal a systematic decline in capacity with increasing current density. At 0.1C, the pouch cell delivered an initial capacity of 2.9 Ah, which slightly decreased to 2.8 Ah after 9 cycles. Similarly, at 0.2C, the capacity ranged from 2.6 Ah initially to 2.5 Ah over the same number of cycles. A further reduction was observed at higher rates: at 1C, the capacity dropped from 1.9 Ah to 1.8 Ah, and at 2C, it decreased from 1.2 Ah to 1.1 Ah. This trend is indicative of increased polarization and kinetic limitations at higher current densities, which result in reduced utilization of the active material. Despite these decreases, the relatively modest capacity fade across nine cycles at each rate suggests that the cell exhibits stable performance under various operational conditions. Overall, the results confirm that while higher C-rates inherently lead to lower discharge capacities, the cell maintains consistent performance, which is promising for its potential application in devices requiring varied power outputs.

Funded by the European Union

Views and opinions expressed are those of the author(s) only and do not necessarily reflect those of the European Union or CINEA. Neither the European Union nor the granting authority can be held responsible for them. This project has received funding from Horizon Europe research and innovation programme under Grant Agreement No.1069890

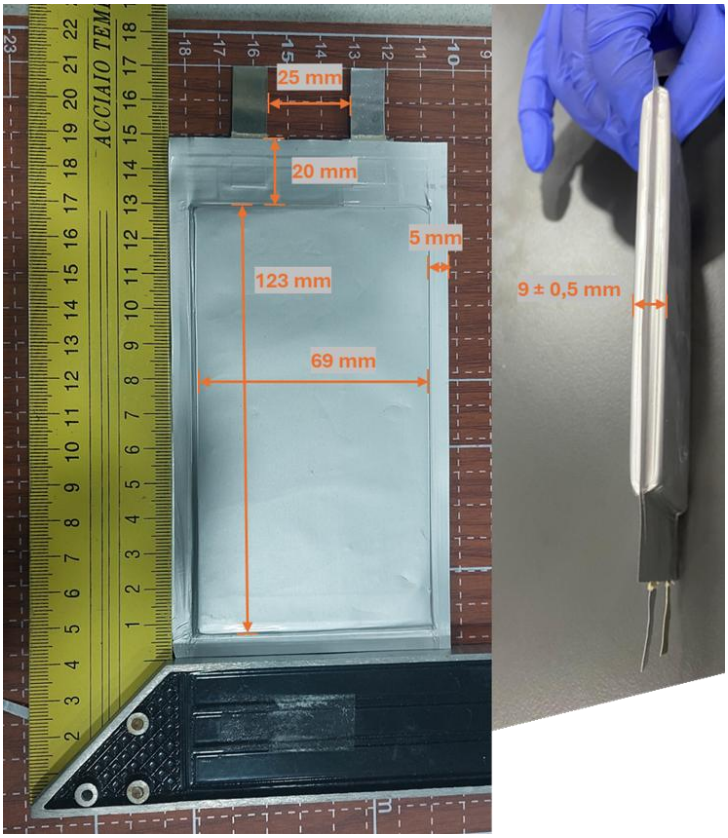

Figure 6.4. *Optical image of the final size pouch cell with specific dimensions*

Figure 6.5. *Digital image of the assembled pouch cell for sending the project partners for pack design*

Funded by the European Union

Views and opinions expressed are those of the author(s) only and do not necessarily reflect those of the European Union or CINEA. Neither the European Union nor the granting authority can be held responsible for them. This project has received funding from Horizon Europe research and innovation programme under Grant Agreement No.1069890

Optimized pouch cells with dimensions of approximately 12 cm x 7 cm have been successfully assembled using commercial materials, achieving an average capacity of 7 Ah. These cells serve as a performance benchmark; following detailed optimization of recycled materials within the project, new pouch cells of identical dimensions will be fabricated and demonstrated. Figure 7.4 shows a pouch cell with all its dimensions, and Figure 7.5 shows the complete set of pouch cells prepared for delivery to the project partner for initial battery pack design. The detailed information and experimental results of this section will be presented in WP4.

7. Conclusions

This deliverable presents a comprehensive evaluation of end-of-life (EOL) lithium-ion battery (LIB) cells, the performance of recycled electrode materials, and the scale-up of pouch cell configurations. The findings contribute to the broader objectives of the FREE4LiB project, supporting the transition toward a circular economy for LIBs by promoting second-life applications and enhancing material recovery strategies.

The electrochemical characterization of EOL cells from multiple sources, including electric vehicles, e-bikes, and e-scooters, was conducted collaboratively by project partners, including FBK, IREC, SAU, and NESSTEC. These tests provided critical data on the state of charge (SOC), state of health (SOH), and overall degradation mechanisms, informing the classification of cells suitable for reuse or recycling. The results highlighted significant variability in the remaining capacity of the tested cells. While some retained over 50% of their initial capacity, others exhibited irreversible degradation. Pack 1 was entirely over-discharged, with all 56 cells measuring 0V, rendering them unsuitable for reuse. Several prismatic cells from Packs 2, 7, and 8 exhibited severe swelling, posing safety risks. Cells from Pack 4, which underwent preconditioning and capacity measurements, demonstrated varying performance, with the highest capacity reaching 1.8 Ah and the lowest measuring 0.9 Ah, confirming the need for detailed screening before second-life applications.

The characterization of EOL cells conducted by FBK provided additional insights into the degradation patterns of different battery modules. FBK tested 30 Kona cells and 4 additional Kona cells from different sources, performing dismantling, standard testing, and aging studies. The preliminary tests revealed significant variations in capacity retention, with aged cells showing increased internal resistance and capacity fade over multiple cycles. Some cells exhibited stable electrochemical behavior, while others displayed severe

Funded by the European Union

Views and opinions expressed are those of the author(s) only and do not necessarily reflect those of the European Union or CINEA. Neither the European Union nor the granting authority can be held responsible for them. This project has received funding from Horizon Europe research and innovation programme under Grant Agreement No.1069890

deterioration, highlighting the importance of module-specific evaluations before deciding on second-life or recycling pathways.

The performance evaluation of lithium-ion cells incorporating recycled cathode materials demonstrated promising potential, though further optimization is required. Half-cell tests showed an initial discharge capacity of 168 mAh/g, which stabilized at 150 mAh/g after five cycles. Full-cell configurations exhibited an initial capacity of 113 mAh/g, decreasing to 105 mAh/g, indicating some level of capacity fade. Additionally, impedance spectroscopy measurements revealed slightly higher internal resistance in cells utilizing recycled materials compared to commercial references, suggesting the need for improved electrode processing and interface stability. While these results confirm the feasibility of integrating recycled materials into new LIBs, further refinements in material recovery and electrode formulation will be necessary to enhance long-term cycling stability.

To bridge the gap between laboratory-scale research and practical applications, lithium-ion cells were successfully scaled up to pouch cell configurations. Initial 300 mAh pouch cells were fabricated using a stacking method and tested under different conditions. The first charge capacity was recorded at 320 mAh, while the initial discharge capacity measured 220 mAh, increasing to 250 mAh in the second cycle, suggesting activation effects. C-rate performance testing showed capacity retention across different current densities, with 2.8 Ah at 0.1C and 1.1 Ah at 2C after nine cycles, highlighting the impact of higher current rates on capacity retention. Following these evaluations, 7 Ah pouch cells with dimensions of 12 cm × 7 cm were fabricated using commercial materials as a benchmark. These large-format pouch cells will serve as a reference for future testing with optimized recycled materials, enabling a direct comparison of their viability for industrial applications.

Overall, the effort in this deliverable underscores the importance of integrating second-life applications with optimized LIB recycling methodologies. The findings confirm that while certain EOL cells retain sufficient capacity for reuse, proper classification is essential to ensure safety and performance. Additionally, while recycled cathode materials show promising electrochemical behavior, further refinements are necessary to enhance their stability and efficiency in practical applications. The successful transition from small-scale to large-format pouch cells represents a crucial step toward industrial feasibility. The results from this deliverable will support WP4 by guiding the development of battery pack designs and re-manufacturing processes, contributing to a more sustainable and resource-efficient LIB industry.

Funded by the European Union

Views and opinions expressed are those of the author(s) only and do not necessarily reflect those of the European Union or CINEA. Neither the European Union nor the granting authority can be held responsible for them. This project has received funding from Horizon Europe research and innovation programme under Grant Agreement No.1069890

Annex A - ST2.2.1 Electrochemical Characterization Procedure

Introduction

This document details the procedure to be used for the electrochemical characterization of cells in the Free4Lib project, within the subtask ST2.2.1.

In the introduction some definitions that will be used along the procedure are listed. First, some general definitions are listed, which corresponding values should be found in the cell datasheet. Second, some experimental definitions are listed, which corresponding values are measured or elaborated during the procedure itself.

General definitions

- Q_n = Nominal cell capacity
- T_min = Minimum safety temperature for cell cycling
- T_max = Maximum safety temperature for cell cycling
- V_n = Nominal cell voltage
- V_min = Minimum voltage for cell cycling
- V_max = Maximum voltage for cell cycling
- C = Current to charge/discharge the cell in 1 hour, corresponding to C-rate=1
- I_cut-off = Cut-off current for CV operations (if not declared, C/20)
- I_chr_st = Charge current for standard cycling (if not declared, 0.3C)
- I_dch_st = Discharge current for standard cycling (if not declared, 1C)
- I_chr_max = Maximum continuous charge current (if not declared and compatible with safety limits, use 0.5C)
- I_dch_max = Maximum continuous discharge current (if not declared and compatible with safety limits, use 2C)
- I_chr_pk = Maximum peak charge current (if not declared and compatible with safety limits, use 1C)
- I_dch_pk = Maximum peak discharge current (if not declared and compatible with safety limits, use 3C)

Experimental definitions

- I_c = Charge current
- I_d = Discharge current
- V = Charge or discharge voltage
- CC : Constant Current (charge or discharge) with a setpoint current and an exit on a voltage limit
- CV : Constant Voltage (charge or discharge) with a setpoint voltage and an exit on a current cut-off
- CC+CV : Combined CC and CV procedure; CC until the CV setpoint is reached, then CV until the current cut-off is reached
- T_chamber = Set-point temperature of the thermal chamber
- T_cell = Measured temperature of the cell
- Q_exp_pre = Experimental capacity measured at 25°C during preconditioning

Funded by the European Union

Views and opinions expressed are those of the author(s) only and do not necessarily reflect those of the European Union or CINEA. Neither the European Union nor the granting authority can be held responsible for them. This project has received funding from Horizon Europe research and innovation programme under Grant Agreement No.1069890

- Q_exp_T = Experimental capacity measured at a specific temperature
- SoC_pre = State of charge calculated with reference to Q_exp_pre
- SoC_T = State of charge calculated with reference to Q_exp_T
- OCV_c = Voltage measurement at very low charging current
- OCV_d = Voltage measurement at very low discharging current
- OCV_avg = Average of OCV_c and OCV_d at the same SoC_pre

Procedure

The procedure starts in unidentified conditions of SoC and SoH of the cell. In case of low SoHs, the behavior of a cell can be very different depending on the test temperature. For this reasons, at each testing temperature it is necessary to measure the cell capacity and define a test-related SoC. To allow reliable postprocessing, it is recommended to record voltage, current, ambient temperature and cell temperature without interruptions along the whole procedure. It is also recommended to set a safety exit on T_cell to avoid exceeding T_max along all the procedure. The symbols §, #, * and [ç] redirect to footnotes providing instructions on recurring actions.

1. Preconditioning

1.1. Set thermal chamber at T_cha = 25°C § #
1.2. Standard charge CC+CV: CC at I_c = I_chr_st until V = V_max, CV at V = V_max, exit I_cut-off *
1.3. Discharge CC: CC at I_d = 0.2C until V = V_min *
1.4. Repeat point 1.2 * (set reference for 100% SoC_pre)
1.5. Repeat point 1.3 (measure Q_exp_pre) *
1.6. Standard charge CC at I_c = I_chr_st, exit SoC_pre = 50% *

2. Open Circuit Voltage

2.1. Standard charge CC+CV: CC at I_c = I_chr_st until V = V_max, CV at V = V_max, exit I=C/100 *
2.2. Discharge CC at I_d = 0.05C, exit V = V_min (record V for OCV_d) + wait 30 mins
2.3. Charge CC at I_c = 0.05C, exit V = V_max (record V for OCV_c) *
2.4. Standard discharge CC at I_d = I_dch_st, exit SoC_pre = 80% *

3. Energy and Capacity

3.1. Standard charge CC+CV: CC at I_c = I_chr_st until V=V_max, CV at V = V_max, exit I_cut-off *
3.2. Discharge CC at I_d = I_dch_st, exit V = V_min + wait 30 mins
3.3. Repeat point 3.1 (set reference for 100% SoC_T) and point 3.2 (measure Q_exp_T in dch)
3.4. [ç] Repeat points 3.1 and 3.2 at different I_d =C/3, C/2 and I_dch_max (2 cycles each)
3.5. Standard charge CC at I_c = I_chr_st, exit SoC_T = 50% *

Funded by the European Union

Views and opinions expressed are those of the author(s) only and do not necessarily reflect those of the European Union or CINEA. Neither the European Union nor the granting authority can be held responsible for them. This project has received funding from Horizon Europe research and innovation programme under Grant Agreement No.1069890

4. Pulse Test & EIS

4.1. Standard charge CC+CV: CC at I_c = I_chr_st until V=V_max, CV at V = V_max, exit I_cut-off *
4.2. Standard discharge CC at I_d = I_dch_st/2, exit SoC_T=80% §
4.3. Discharge pulse CC at I_d=0.2C, exit after t = 10 seconds *
4.4. Charge pulse CC at I_c=0.2C, exit after t = (I_d / I_c)·10 seconds *
4.5. Repeat points 4.3 and 4.4 at I_d = 1C, 2C, I_dch_pk and I_c = 1C, I_chr_pk, I_chr_pk, respectively
4.6. Potentiostatic EIS with voltage excitation of 10mV and frequency range [1mHz - 100kHz] *
4.7. Standard Discharge CC at I_d = I_dch_st/2, exit SoC_T = 50% §
4.8. Repeat points 4.3, 4.4, 4.5 and 4.6
4.9. Standard discharge CC at I_d = I_dch_st/2, exit SoC_T = 20% §
4.10. Repeat points 4.3, 4.4, 4.5 and 4.6
4.11. Standard charge CC at I_c = I_chr_st, exit SoC_T=50%

5. Temperature

5.1. Set thermal chamber at T_chamber = 5°C §
5.2. Apply Sections 2, 3 and 4
5.3. Set thermal chamber at T_chamber = 40°C §
5.4. Apply Sections 2, 3 and 4

§ + wait until T_cell = T_chamber or ambient temperature ± 2°C (approx. 1h)
# This step can be skipped if the test is performed at ambient temperature
* + wait 5 minutes
[ç] Apply these steps for extensive testing only

This test procedure must always be adapted not to exceed the voltage, current and temperature safety ranges specified in the cell datasheet. If any value in the procedure exceeds the cell safety range, use instead the range limiting value from datasheet. The adaptation of the procedure to comply with rules and common sense on laboratory safety is responsibility of the test operator.

Funded by the European Union

Views and opinions expressed are those of the author(s) only and do not necessarily reflect those of the European Union or CINEA. Neither the European Union nor the granting authority can be held responsible for them. This project has received funding from Horizon Europe research and innovation programme under Grant Agreement No.1069890